Marine Geology 381 (2016) 67–86

Contents lists available at ScienceDirect

Marine Geology

journal homepage: www.elsevier.com/locate/margo

Sediment dynamics and hydrographic conditions during storm passage, Waquoit Bay, Massachusetts

Christopher V. Maio [a,*], Jeffrey P. Donnelly [b], Richard Sullivan [b], Stephanie M. Madsen [b], Christopher R. Weidman [c], Allen M. Gontz [d], Vitalii A. Sheremet [e]

[a] University of Alaska Fairbanks, Department of Geosciences, PO Box 755780, Fairbanks, AK 99775, USA
[b] Woods Hole Oceanographic Institution, Coastal Systems Group, 266 Woods Hole Road, Mail Stop #22, Woods Hole, MA 02543, USA
[c] Waquoit Bay National Estuarine Research Reserve, 149 Waquoit Highway, Waquoit, MA 02536, USA
[d] University of Massachusetts-Boston, School for the Environment, 100 Morrissey Blvd., Boston, MA 02125, USA
[e] University of Rhode Island, Graduate School of Oceanography, 215 South Ferry Road, Narragansett, RI 02882, United States

ARTICLE INFO

Article history:
Received 16 November 2015
Received in revised form 28 June 2016
Accepted 29 July 2016
Available online 31 July 2016

Keywords:
Sediment dynamics
Storm surge
Irene
Waquoit Bay
Bottom current
Sediment transport

ABSTRACT

The impact of storm events on the sediment dynamics of the shallow groundwater fed estuaries of Cape Cod, Massachusetts, USA is little understood. To address this, the objectives of this study are to assess sediment dynamics during storm passage and determine whether shallow back-barrier lagoons like Waquoit Bay have the preservation potential for a sedimentary archive of hurricanes. When setting out in this study, it was unclear whether paleotempestological methods could be applied successfully to cores collected from the landward reaches of shallow estuaries of southern New England. Water level and bottom current data using Arm-and-Float tide gauges and SeaHorse Tilt Current Meters was collected during Tropical Storm Irene (2011) and coupled with storm surge modeling projections to better elucidate storm-induced sediment transport mechanisms. Three sediment cores were collected at the head of Waquoit Bay, located 2.8 km from the barrier beach. Grain size analysis of sediment cores was conducted with a laser particle size analyzer at 1 cm increments in order to identify coarse grain anomalies, which can act as a storm event proxy. Bayesian statistics were applied to develop age models of two of the cores based on three Pb pollution chronomarkers and 21 continuous flow ^{14}C AMS ages. The results yield variable sediment accumulation rates between 2 mm/yr to 10 mm/yr, with significantly higher rates occurring in the upper 1 m of sediments. Grain size results are highly variable, and contain numerous large amplitude, short duration fluctuations suggesting that during storm passage coarse sand is deposited in the coring site. The sensitivity of the site to both tropical and extratropical storm events, uncertainties in the age model, and the multiple sediment sources and transport pathways limits the utility of using the Waquoit sediments to determine long-term hurricane frequencies. Results nonetheless provide insights into how extreme storm events impact coastal lagoons.

1. Introduction

1.1. Background

For millennia extreme storm events have impacted the New England coastline resulting in catastrophic alterations of coastal systems with significant loss of life and resources (Ludlum, 1963; Boose et al., 2001; Donnelly et al., 2001; Emanuel, 2005; Boldt et al., 2010; Maio et al., 2014, 2015). The dramatic rise in coastal populations during the 20th century (Kelley et al., 1989), coupled with increasing rates of sea-level rise (SLR) (Pachauri et al., 2014; FitzGerald et al., 2008; Kemp et al., 2009), is resulting in increasing vulnerability of millions of people and critical infrastructure along the U.S. northeast coast to future storm events (Kirshen et al., 2007; Woodruff et al., 2013; Brandon et al., 2014). Due to these factors it is important to gain a better understanding of how storm events impact sediment and hydrographic conditions within lagoon systems along populated coastlines.

The environmental role of episodic storm events can only be understood by assessing their individual and collective impacts over centennial to millennial temporal scales and at both local and regional spatial extents. This can be achieved by examining the sedimentary records and incorporating hydrographic measurements and storm surge modeling. A short instrumental and incomplete historical record make understanding long-term trends in storminess difficult, and necessitates the development of paleo-proxy records based on sedimentary data that identify prehistoric storm induced coarse grain event beds (Liu and

* Corresponding author.
E-mail addresses: cvmaio@alaska.edu (C.V. Maio), jdonnelly@whoi.edu (J.P. Donnelly), rsullivan@whoi.edu (R. Sullivan), smadsen@whoi.edu (S.M. Madsen), chris.weidman@state.ma.us (C.R. Weidman), allen.gontz@umb.edu (A.M. Gontz), vsheremet@whoi.edu (V.A. Sheremet).

http://dx.doi.org/10.1016/j.margeo.2016.07.004
0025-3227/

Fearn, 2000; Donnelly et al., 2001, 2015; Buynevich et al., 2004; Boldt et al., 2010; Lane et al., 2011; Brandon et al., 2014). The study of prehistoric tropical cyclones based on geologic proxies and historical records, known as "paleotempestology," provides methods to address this gap in knowledge by elucidating local sediment dynamics during storm passage and providing late Holocene chronologies of hurricane events (Emanuel, 1988; Nott, 2004; Nott et al., 2007; Woodruff et al., 2008: Wallace et al., 2014). Previous paleotempestological studies have shown that sedimentary archives of past hurricane events have been well preserved in some back-barrier environments as coarse grain horizons interbedded with finer sediments (peat, mud, and silt) (Emery, 1969; Liu and Fearn, 1993; Donnelly et al., 2001, 2015; Donnelly and Woodruff, 2007; Scileppi and Donnelly, 2007; Woodruff et al., 2008; Brandon et al., 2014). However, not all locations are suitable for storm reconstructions and therefore efforts to identify viable study sites is an important component to advancing the science (Wallace et al., 2014).

An important component for determining the feasibility of applying paleotempestological methods to the shallow groundwater fed estuaries of Cape Cod is developing a better understanding of the sediment dynamics operating during storm passage. This study will address three questions in regard to the Waquoit Bay lagoon system including:

1) During extreme storm events what are the hydrographic conditions impacting sediment transport pathways?

2) What are the sediment sources and transport pathways that contribute to coarse sand deposition within the north basin?

3) Do the sediments in the north basin archive a record of past storm events that can be used to calculate long-term hurricane frequencies?

1.2. Regional setting

Waquoit Bay is located on the south shore of Cape Cod within the towns of Falmouth and Mashpee, Massachusetts, approximately 90 km southeast of Boston (Fig. 1). The geologic framework of the lagoon consists of reworked glacial sediments. During the end of the Wisconsin Glacial Period, the Laurentide Ice Sheet reached its southern terminus at the islands of Nantucket and Martha's Vineyard approximately 23,000 ybp (Balco and Schaefer, 2006). The subsequent coastal evolution of southeast Massachusetts occurred in response to the melting and northward retreat of the ice sheet beginning approximately 18,000 ybp (Gutierrez et al., 2003; Oldale, 1992; Uchupi and Mulligan, 2006). Flow of meltwater resulted in the formation of a pitted outwash plain consisting mostly of sand, which became deposited around and above the stagnant ice blocks and ice contact debris (Uchupi and Mulligan, 2006). Groundwater seepage along the southern end of the outwash plain resulted in the formation of linear spring sapping valleys, which sometimes crossed the kettles and reworked the existing outwash deposits (Gutierrez et al., 2003). The relict glacial topography including the kettles and spring sapping valleys have been subsequently altered by fluvial, coastal, and aeolian processes and provides the geologic framework for the Waquoit system (Oldale and O'Hara, 1984; Gutierrez et al., 2003; Uchupi and Mulligan, 2006).

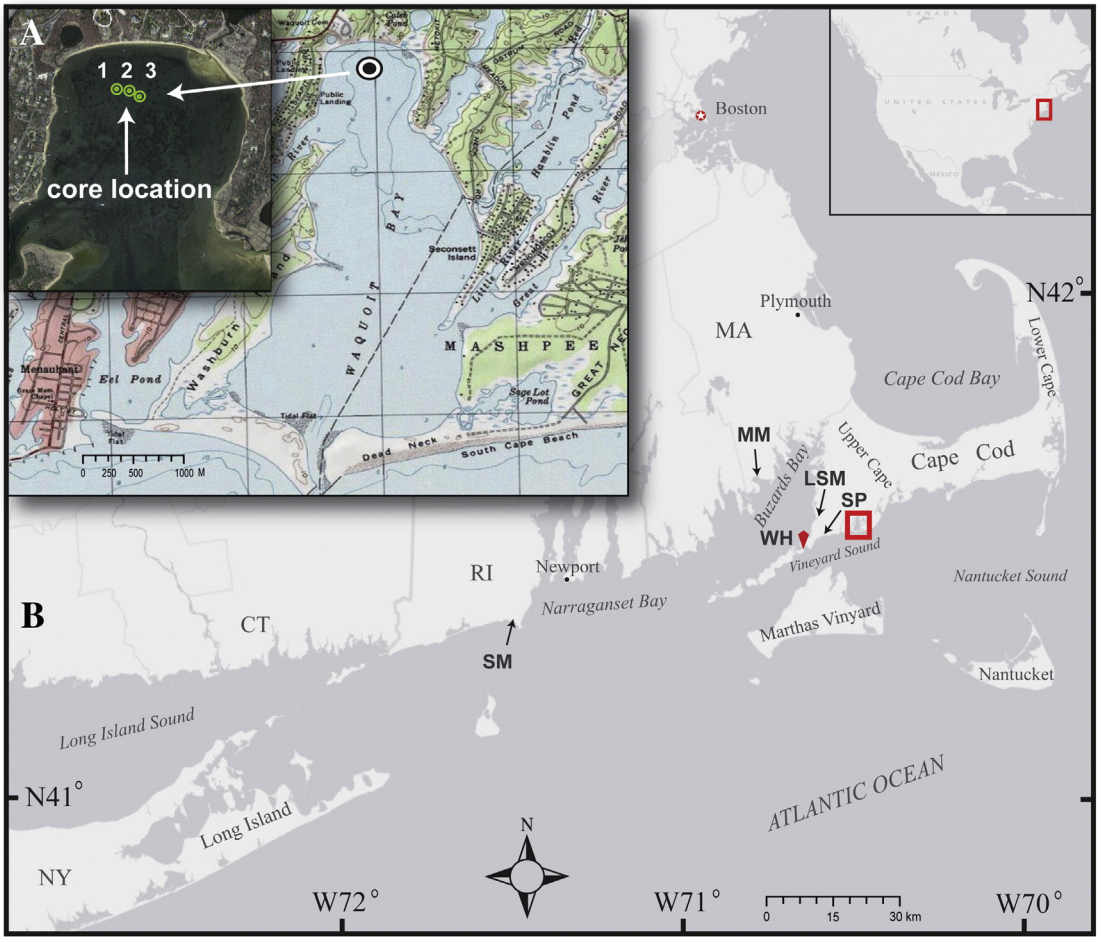

Fig. 1. The study site is located within Waquoit Bay, a shallow water estuary along the south shore of Cape Cod, Massachusetts, USA. A) The three sediment cores (WAQ1, WAQ2, and WAQ3) were collected in the north basin of the bay approximately 50 m apart. B) The lagoons position along the south side of Cape Cod, and its south to north orientation makes it particularly sensitive to storm surges resulting from northward tracking hurricanes. The Woods Hole (WH) tide gauge provides instrumental records of storm surges going back to 1932. The location of previous storm reconstructions carried out in the area (i.e. Donnelly et al., 2001; Madsen et al., 2009; Boldt et al., 2010; Donnelly et al., 2015) include Succotash Marsh (SM) Mattapoisett Marsh (MM), Little Sippewissett Marsh (LSM) and Salt Pond (SP) respectively.

Currently, Waquoit Bay reaches a maximum depth of 3 m, encompasses an area of 3.7 km^2, and has a mean tidal fluctuation of approximately 0.79 m (Maio et al., 2014). Waquoit Bay is fronted on its southern end by a barrier complex made up of South Cape Beach, Dead Neck, and Washburn Island. The estuary receives tidal influx from adjacent Vineyard Sound at its southern end through the navigable channel located between Dead Neck and Washburn Island. Further to the west along Washburn Island, a smaller and historically ephemeral inlet (Aubrey et al., 1993; Valiela et al., 1998), provides tidal influx into the Eel Pond sub-estuary, which is linked to Waquoit Bay's north basin through the Seapit River (Rosen, 2003).

The main bay is connected to smaller sub-estuary lagoon and saltmarsh systems including Eel Pond, Child's River and the Seapit River to the west and Hamblin and Jehu Ponds to the east (Fig. 1). The estuary primarily receives freshwater input through groundwater seepage (Fox et al., 2012) and to a lesser degree Red Brook, and the Quashnet River. None of these stream systems flow directly into the north basin of Waquoit Bay and given the small size of the Waquoit catchment, highly permeable sandy soils, and low inland topographic gradient, their impact on the transport and deposition of sand within the north basin is assumed to be minimal.

Waquoit Bay is characteristic of numerous other shallow micro-tidal lagoon systems on the northeastern U.S. coastline. Attributes that characterize these systems include a sand dominated relict glacial topography, the presence of barrier beaches and back-barrier salt ponds and marshes, freshwater inputs dominated by groundwater seepage, and a shallow water depth and low topographic gradient moving inland (WBNERR, 2016). Additionally, many of these areas have experienced a rapid increase in coastal development and recreational activities during the past 50 years (WBNERR, 2016).

Our initial selection of Waquoit Bay as our coring location was based in-part on the fact that it is characteristic of other systems in the region. This allows for us to make some regional assertions based on our local results. The presence of the Waquoit Bay National Estuarine Research Reserve (WBNERR) was also a factor as there have been numerous studies carried out at the site and the information gained by the work contributes to the overall understanding of storm impacts within the reserve (WBNERR, 2016).

The coring location was also selected based on the lagoons southern orientation making it susceptible to storm surges associated with northward tracking hurricanes while at the same time buffered from the northeast winds associated with Nor'easters (Boldt et al., 2010). This factor is important as one of our objectives was to determine whether a sediment-derived chronology of hurricane events was preserved, a task that is complicated when extra-tropical storms also impact the site. Based on our review of historical and instrumental records, between 1635 and 2011 there were approximately 17 hurricanes and 3 Nor'easters that caused significant coastal damage to the south facing beaches of Cape Cod (Snow, 1943; Ludlum, 1963; Boose et al., 2001) (Table 1). It is likely that other tropical and extratropical storms also impacted the region but the early historical accounts are spatially sparse and often lacking details.

In New England, extra-tropical winter storms have resulted in similar magnitude storm surges as hurricanes, but typically only along eastern and northeastern facing shorelines (Snow, 1943; Dickson, 1978; Donnelly et al., 2001). During winter storm events, known locally as Nor'easters due to the prominent winds blowing from the northeast, the southern facing beaches of Cape Cod are relatively buffered from the heavy winds when compared to hurricanes. The limited fetch distance and exposure during these events hinders the ability of large storm surges to form (Boldt et al., 2010). However, it should be noted that despite extra-tropical storms often having offshore winds, these long duration events can drive internal circulation changes that could alter sediment transport pathways, especially in shallow water lagoons. An extreme example is provided by the notoriously devastating Blizzard of '78. During the storm a surge of 3 m was recorded in the north facing Boston, while a surge of 1.3 m at the southern facing Woods Hole (NOAA, 2016). Despite the difference, a 1.3 m storm surge at Woods Hole is comparable to those experienced during major hurricane events.

Table 1
Major tropical and extra-tropical storm events impacting southeastern Massachusetts between 1635 and 2011 (Snow, 1943; Ludlum, 1963; Boose et al., 2001).

Year	Storm event	Landfall date	Landfall location	Saffir Simpson scale
2011	Irene	28-Aug	NY City	Cat 1
1991	Bob	19-Aug	Newport	Cat 2
1991	Perfect Storm	1-Nov	Cape Cod	Nor'easter
1985	Gloria	4-Sep	CT	Cat 1
1978	Blizzard of '78	7-Feb	New England	Nor'easter
1976	Belle	10-Aug	Long Island	Cat 1
1976	Groundhog Day Storm	2-Feb	New England	Nor'easter
1960	Donna	5-Sep	Long Island	Cat 1
1954	Edna	11-Sep	Cape Cod	Cat 1
1954	Carol	31-Aug	Long Island - CT	Cat 2
1944	Great Atlantic Hurricane	15-Sep	Long Island	Cat 2
1938	Great New England Hurricane	21-Sep	Long Island	Cat 3
1869	The September Gail	8-Sep	CT- RI boarder	*Cat 2
1841	The October Gail	3-Oct	East of Nantucket	*Cat?
1815	Great September Gail	23-Sep	Long Island	*Cat?
1770	The Late Season Storm of 1770	20-Oct	Southeast New England	*Cat?
1761	The Southeast New England Hurricane	23-Oct	MA	*Cat?
1727	A Great Rain and Horrible Wind	27-Sep	MA	*Cat 3
1638	Unnamed	13-Aug	RI	*Cat 3
1635	The Great Colonial Hurricane	25-Aug	RI	*Cat 4

1.3. Land use

Historic and modern land uses are important to consider when assessing the sediment dynamics of Waquoit Bay. Prior to European colonization, ancient Native Americans from the Wampanoag tribe had lived and harvested resources in the Waquoit area for over 3000 years (Bell, 2009; Cronon, 2011; Maio et al., 2013). The establishment of the Plymouth Colony in 1620, and eventually the Massachusetts Bay Colony in 1628, led to the influx of thousands of European settlers forever changing the Cape Cod environment (Cronon, 2011; Bell, 2009). Between 1675 CE and 1750 CE the upland forests surrounding Waquoit Bay were cleared to make way for large farms and grazing pastures and by the end of the 19th century much of the inland wetlands had been converted for cranberry agriculture, which prospered due to the areas sandy soils (Orson and Howes, 1992). These anthropogenic changes led to increased sediment loads entering many of the area's coastal lagoons altering sediment dynamics that had operated for millennia (Cronon, 2011; Orson and Howes, 1992; Donnelly et al., 2015).

In 1930, the U.S. Army Corps of Engineers dredged and stabilized the natural entrance into Waquoit Bay, fortifying it with large stone jetties (Keay, 2001). During the same decade, mosquito ditching was aggressively carried out in most of the area's salt marshes (Orson and Howes, 1992). When these factors were coupled with accelerated rates of SLR, there were significant changes to sediment transport and plant community structure within the estuary (Orson and Howes, 1992). In the early 1940s, the U.S. Army began extensive use of the barrier beaches and island fronting Waquoit Bay as a secret training grounds for amphibious landings in preparation for the D-Day Invasion (Keay, 2001). During this time the western inlet connecting Eel Pond to the Vineyard Sound, which opened during the 1938 Hurricane, was filled and fortified by the U.S. Military. This inlet was again temporarily breached during the 1991 Hurricane Bob (Valiela et al., 1998). Slated for development in the 1970s after decades of neglect, the area was established as a State Park and in 1988, through community action,

was incorporated into WBNERR. The reserve contains nearly 1000 ha of protected coastal lands designated for research, education, and recreation (WBNERR, 2016).

2. Methods and materials

One of the primary objectives of this study was to determine the influence of storm events on sediment transport and deposition within the north basin and assess the feasibility of calculating a long-term record of hurricane frequencies. Achieving these objectives requires the application of variety of methods including measuring hydrographic conditions during storm passage. Data obtained from water level gauges and current meters deployed during the 2011 Tropical Storm Irene, combined with storm surge modeling of modern and historical hurricane events, will help to resolve the conditions responsible for the deposition of sand within the north basin and identify which events would have been most likely to leave a geologic signature of their passage.

To determine the rate and character of sediment deposition and its relation to storm passage, grain size analysis coupled with age modeling are employed. Bulk lead (Pb) pollution chronomarkers and radiocarbon aged macrofossils are utilized to determine the age-depth relationship within the cores. When this information is integrated with instrumental observations and historical accounts of storm events impacting Waquoit Bay (Table 1), it can be determined whether there is a connection between grain size anomalies and storm passage in the upper portions of the cores. This information can then be used to interpret long-term trends and determine whether it's possible to calculate long-term hurricane frequencies.

2.1. Hydrographic data

To help decipher the mechanisms of sediment transport and deposition during storm events an array of nine SeaHorse Tilt Current Meters and a series of Arm-and-Float tide gauges were deployed a few days prior to Tropical Storm Irene (2011) for a period of one week (Fig. 2). Irene was a strong Category 1 hurricane when it made landfall in Brooklyn, New York and caused widespread damage across the East Coast including coastal erosion and flooding (Avila and Cangialosia, 2011). Once Irene made landfall it was downgraded to a tropical storm and impacted Waquoit as such (Avila and Cangialosia, 2011).

The current meter array was placed along the lagoon's major north-south axis in approximately 2.5 m to 3 m of water and provided an estimate of average current velocities occurring within the bottom portion of the water column. The water level instruments were deployed at several locations including near the main channel into Waquoit Bay and in the northern part of the Seapit River, adjacent to the north basin (Fig. 2C). Similar instruments were successfully deployed on lobster traps in the Gulf of Maine and used for analysis of near bottom circulation

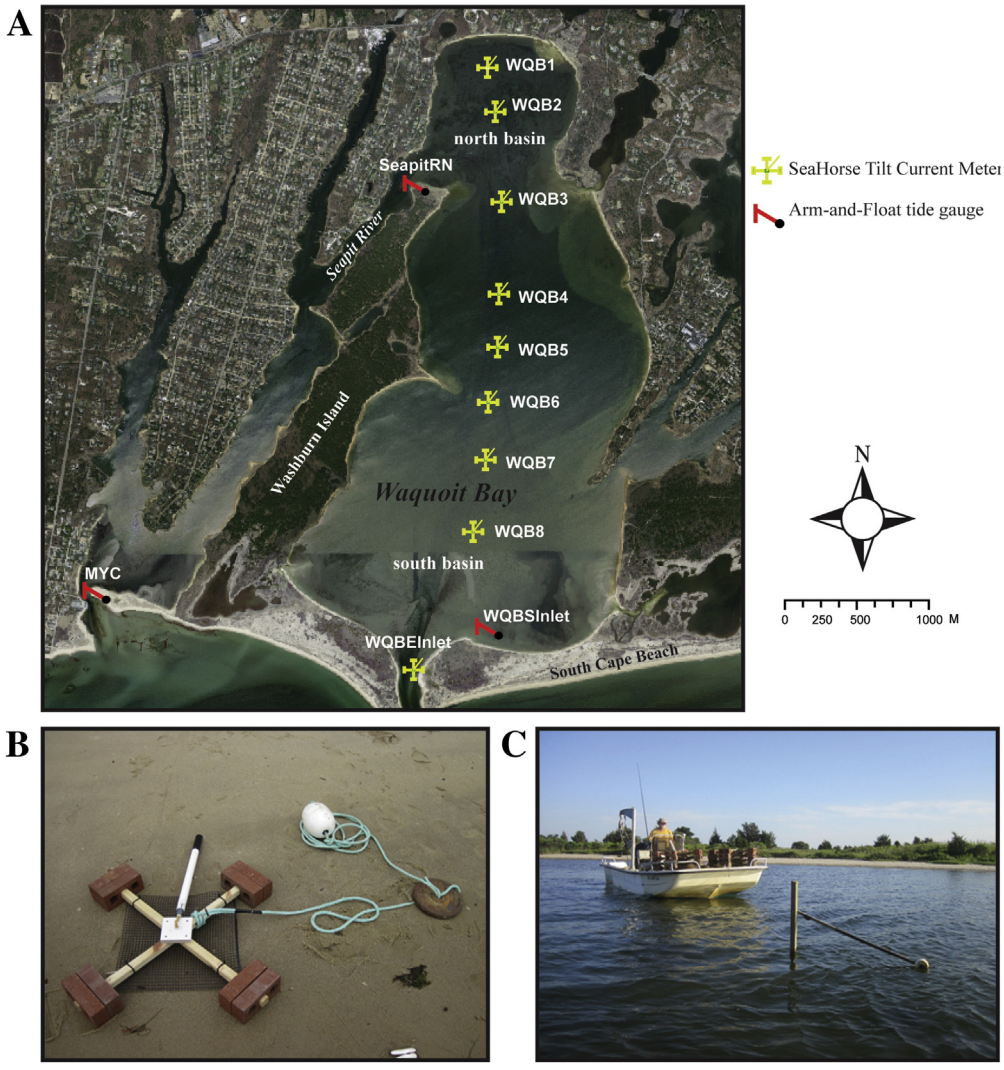

Fig. 2. A) Array of SeaHorse Tilt Current Meters and Arm-and-Float tide gauges placed in the bay prior to Tropical Storm Irene. B) Current meter attached to a cross-shaped mooring base with a line to a secondary weight and a surface buoy prior to deployment. C) Water level gauge deployed in the South Basin of Waquoit Bay near the main inlet (WQBSInlet).

and sediment transport (Aretxabaleta et al., 2013). Hydrographic data will aid in the identification of the location and direction of high velocity currents capable of transporting sand into the coring site.

2.2. Modeling storm surges at the site

Accurately determining the surge elevations within Waquoit Bay during hurricanes documented in the instrumental and historical record was a necessary component to understanding depositional patterns and correlating a particular storm event to an observable sand horizon in the core. Upon beginning this research, the only information regarding the character and elevation of storm surges within Waquoit Bay was limited to a few studies looking at the morphologic and ecological impacts of Hurricane Bob in 1991 (i.e. Aubrey et al., 1993; Valiela et al., 1998). For hurricanes prior to 1991, only anecdotal accounts of water levels were available.

In order to estimate the storm surge in Waquoit Bay from historical hurricanes, hindcast surge modeling was carried out using the Sea, Lake and Overland Surges from Hurricanes (SLOSH) model (Jelesnianski et al., 1992). SLOSH provides an estimate of storm surge heights using a set of meteorological parameters including atmospheric pressure, storm size, forward speed, and track data (Jelesnianski et al., 1992). When integrated with local bathymetric and topographic data, SLOSH can accurately model storm surge height within individual grid cells located in the model domain (Jelesnianski et al., 1992). Surges were modeled for select modern and historical storms at both the Woods Hole tide gauge and within Waquoit Bay, allowing for a direct comparison between observed and modeled storm tides at Woods Hole and serving as validation of model parameters. Surge values were adjusted to account for the position of the astronomical tide at landfall and made relative to the mean high high water (MHHW) datum. Unfortunately, SLOSH is only able to model tropical cyclones and not extratropical events due to the different storm characteristics.

2.3. Field work

Three sediment cores were obtained within the north basin of Waquoit Bay using either an Oztec vibracore system (Lanesky et al., 1979) or a Rossfelder Corp's P-3 vibro-percussive system deployed from a modified 20 ft pontoon boat. The core sites were located within the deepest portion of the bay at water depths ranging from 2.5 to 3 m. Core locations were spaced ~50 m apart along an east – west transect. Cores were collected in 7.6 cm ID aluminum barrels. Core WAQ1 (recovered length of 6 m) was obtained in August of 2011. Cores WAQ2 and WAQ3 were obtained in June of 2012 using a combination of the Oztec driven vibracore for the first 4 m followed by a Rossfelder vibro-percussive system until the point of refusal was reached (8.41 m and 8.27 m, respectively).

2.4. Sedimentary analysis

Sediment cores were split, photographed, and described by sediment type, texture, grain size, character of the transitions between horizons, and color. Grain size analysis using a Beckman Coulter laser diffraction particle size analyzer was carried out at continuous 1 cm intervals. We identified coarse grain anomalies within the Waquoit cores based on sedimentary characteristics and anomalously high D90 grain size. D90 is the grain size of which 90% of all other sediments in the sample fall below in size, thus identifying the coarsest 10% of the total sample. Typical estuarine deposition within the north basin of Waquoit Bay is dominated by fine-grained organic rich sandy mud mixed with fine to medium sand, while distal barrier and proximal bluff and shoreline sediments consist primarily of well sorted and rounded medium to coarse sands. Based on previous studies carried out in coastal ponds and lagoons (i.e. Emery, 1969; Liu and Fearn, 1993; Woodruff et al., 2008; Donnelly et al., 2015), we hypothesize that these coarse grain intervals provide a signature of a rapid and episodic onset of high transport energy characteristic of storm events. Based on the geography of Waquoit and the limited carrying capacity of area streams, a flood event derived from the Childs and Quashnet Rivers was ruled out as a possible source of coarse grain deposition within the north basin.

It was necessary to filter the grainsize data to remove long-term variability that occurs on timescales much greater than individual events that would have made interpretation difficult. A filtering method was applied to the three cores to identify sample to sample excursions from background sedimentation. In this method, a sliding 20-year running average (based on the age model) of D90 grain size was subtracted from the centimeter interval falling directly above (Lane et al., 2011). For example, within WAQ1 the average D90 taken from the proceeding 20 year (~4–16 cm depending on sedimentation rate) interval was subtracted from the raw D90 grain size falling within the centimeter interval directly above. This method removes detection biases resulting from low frequency changes in background sediment composition (Lane et al., 2011). This resulted in both positive and negative anomalies. Positive values served as the proxy for increased transport energy within the system assumed to be brought about by storm passage.

2.5. Age control

To develop an age model radioisotope, bulk lead (Pb), and radiocarbon, dating methods were applied. A high resolution germanium well gamma detector was used to detect ^{210}Pb and ^{137}Cs activity at discrete intervals ranging from 1–5 cm in the uppermost meter of sediments from WAQ1. The analysis of lead (Pb) concentrations with sediment depth was carried out using an ITRAX X-Ray florescence (XRF) core scanner. Lead pollution has been well documented within northeastern U.S. sediments, rapidly increasing above background levels as a result of the Industrial Revolution between 1850 CE and 1900 CE (Nixon, 1995; Legra et al., 1998). In addition to the pollution chronomarkers, 21 macrofossil bivalve and gastropod samples were selected from the WAQ1 and WAQ2 cores for continuous flow atomic mass spectrometry (CFAMS) ^{14}C dating (Roberts et al., 2011). This new and low cost continuous flow AMS (CFAMS) method is capable of directly analyzing CO_2 gas and, hence, skips the conversion to graphite process (Roberts et al., 2013). The major drawback is that uncertainties with dates can be as much as 6 times greater than traditional AMS methods (approximately ± 150 compared to ± 25). Constrained by a low research budget, we elected to age all samples utilizing the CFAMS method.

All samples were submitted to the Woods Hole Oceanographic Institution National Ocean Sciences Accelerator Mass Spectrometry (NOSAMS) facility. All radiocarbon ages were calibrated using Calib version 7.0.1 with the Marine13 calibration data set (Reimer et al., 2013). With no direct estimates of ΔR from Waquoit Bay available we use the regional estimate of ΔR of -95 ± 45 in this study (Stuiver and Braziunas, 1993; Little, 1999). This ΔR is based on work carried out in southeast Massachusetts by Little (1993), who used paired marine and terrestrial ages from coastal archaeological sites to determine an accurate reservoir correction for the area. Little's work confirmed the earlier methodologies applied by Stuiver et al. All ^{14}C and other age model derived dates are reported in calibrated years before present (cal BP) and calibrated years AD/BC (AD or BC) with a 1 sigma (1σ) range of uncertainty.

To determine sediment accumulation rates age-depth modeling was carried out using an open-source software called “Bacon” (Blaauw and Christen, 2011). Bacon uses Bayesian statistics to determine accumulation histories for deposits and is able to integrate radiocarbon, pollution chronomarkers, and prior information. This method works particular well when compared to linear regression modeling in areas where sedimentation rates have fluctuated through time as prior assumptions about accumulation rates and their variability through time is explicitly taken into account (Blaauw and Christen, 2011).

3. Results

3.1. Hydrographic data

Results from the deployment of the current meter and water level gauges indicate that during Irene there was a marked change in hydrographic conditions within Waquoit Bay. The Seapit River (SeapitRN) water level logger recorded a maximum storm tide of 0.37 m above MHHW concurrent with the passage of the low pressure anomaly. Water levels at this location were 13 cm greater than that observed at the more seaward south basin site (WQBSInlet) indicating a build-up of surging waters at the head of the bay (Fig. 3). The higher water levels were synchronous with the low pressure anomaly and maximum wind speeds (Fig. 4). We ruled out precipitation driven run-off and stream flow as major contributors to higher water levels recorded at the northern outlet of the Seapit River (SeapitRN) adjacent to the north basin. Increased flow down the small streams entering Waquoit Bay would have had a significant lag time after the passage of the low pressure anomaly when the higher elevations were measured. Furthermore, rainfall did not significantly impact the area until the following day when Irene moved inland (Avila and Cangialosia, 2011).

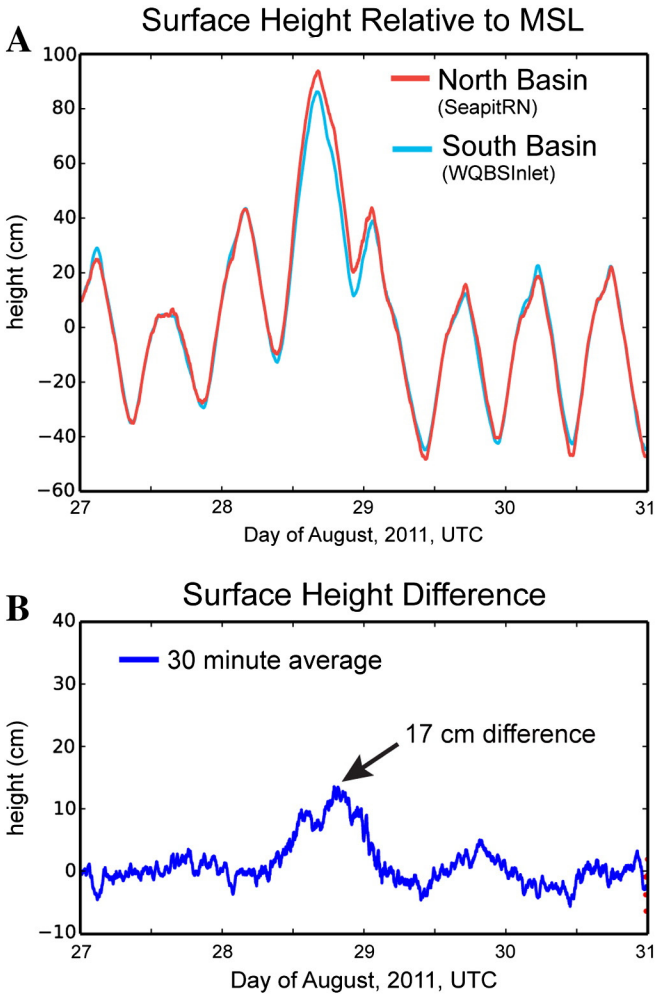

Fig. 3. Storm surge heights mean sea level (MSL) recorded by water level instruments during Tropical Storm Irene. A) Water levels recorded by the WQBSInlet station located within the south basin (blue line) and by the SeapitRN station (red line) located adjacent to the north basin. B) The thirty minute average of water level difference between the two water level gauges documenting increased water levels at landward reaches of the lagoon. (For interpretation of the references to color in this figure legend, the reader is referred to the web version of this article.)

During the height of Irene, high winds and a low pressure anomaly (Fig. 4A) were synchronous with a peak in bottom current velocities within the lagoon (Fig. 4B). The strongest currents (75 cm/s) were recorded by WQBInlet within the main channel at the southern end of the lagoon. The northernmost site (WQB1) at the head of the bay recorded the second fastest currents, with a strong alongshore eastward current moving at 25 cm/s, later, with a change in wind direction, reversing to 15 cm/s westward flowing current. Additionally, WQB1 recorded a 10 cm/s offshore southward flowing component. The current magnitudes between WQB1 and WQB2 were similar, with WQB1 being closer to shore exhibiting a stronger along-shore component. We note that the near-bottom currents measured by the SeaHorse Tilt Current Meters should neither be directed along the wind as the wave-driven flow suggests nor to the right of the wind as the Ekman theory suggests. Rather, the near bottom velocities show significant components in the direction opposite to the wind as surface waters pile up along the windward shoreline (Geyer, 1997).

3.2. Storm surge modeling

SLOSH was utilized to derive storm surge values for eleven modern and historic storms at both the Woods Hole tide gauge and within Waquoit Bay (Table 2). Modeling these events and comparing them to instrumental observations allows us to accurately identify hurricane events that would have significantly impacted the transport and deposition of coarse sediments within Waquoit Bay. Tidal corrections obtained from the Woods Hole tide gauge were applied to SLOSH outputs from the five most recent storms allowing for the calculation of the storm tide height relative to MHHW (NOAA Tides and Currents, 2014). In the instances when tide gauge data was unavailable, NOAA provides hind cast predictions of the approximate time and magnitude of the high and low tides at any given day (NOAA Tides and Currents, 2014). For the 1635 hurricane hindcast tide data was unavailable and tidal corrections were not applied. Tidally correcting the SLOSH surge outputs allows for a more accurate depiction of the storm tide during the event. In all but one case, for events occurring within the instrumental period, the modeled surge heights at Woods Hole are consistent with observed (tide gauge derived) heights validating the SLOSH methodologies and selected parameters. 1954s Hurricane Carol had an observed storm surge of 2.55 m, though model outputs resulted in a surge of 1.71 m. Given the degree to which the other models matched the observation record it's possible that the discrepancy with Carol lies in the Best Track or Tide Gauge data (Boldt et al., 2010). Additionally, water level data recorded during Irene (2011) within Waquoit Bay further validates SLOSH results with an observed storm tide height of 0.50 m above MHHW and modeled height of 0.37 m.

The greatest magnitude storm surge modeled was the Great Colonial Hurricane of 1635 (Fig. 5). Within Waquoit Bay, the modeled results yield a storm surge of 3.05 m, while at Woods Hole the modeled value was 3.72 m of surge. SLOSH results from the Great September Gail of 1815 resulted in a surge of 2.04 within Waquoit Bay, making it the second highest surge of the model runs. The most recent major hurricane to strike Cape Cod was Bob (1991), a Category 2 storm that caused significant coastal damage within Buzzards Bay and the southern facing beaches of Cape Cod (Valiela et al., 1998). The SLOSH model of Bob produced a storm surge of 1.62 m at Waquoit Bay (equating to a storm tide of 1.39 m) (Fig. 5). Other events such as Hurricanes Gloria (1985), Bella (1976), and Donna (1960) all resulted in less than a 1 m storm tide.

3.3. Core stratigraphy

Stratigraphy of the three cores has been divided into three main facies identified here as Units A, B, and C (Fig. 6). Unit A is confined to the uppermost sediments and is primarily composed of organic rich, gelatinous mud having a dark brown color. This unit is marked by a number of articulated marine bivalves making bioturbation likely. Radiographs

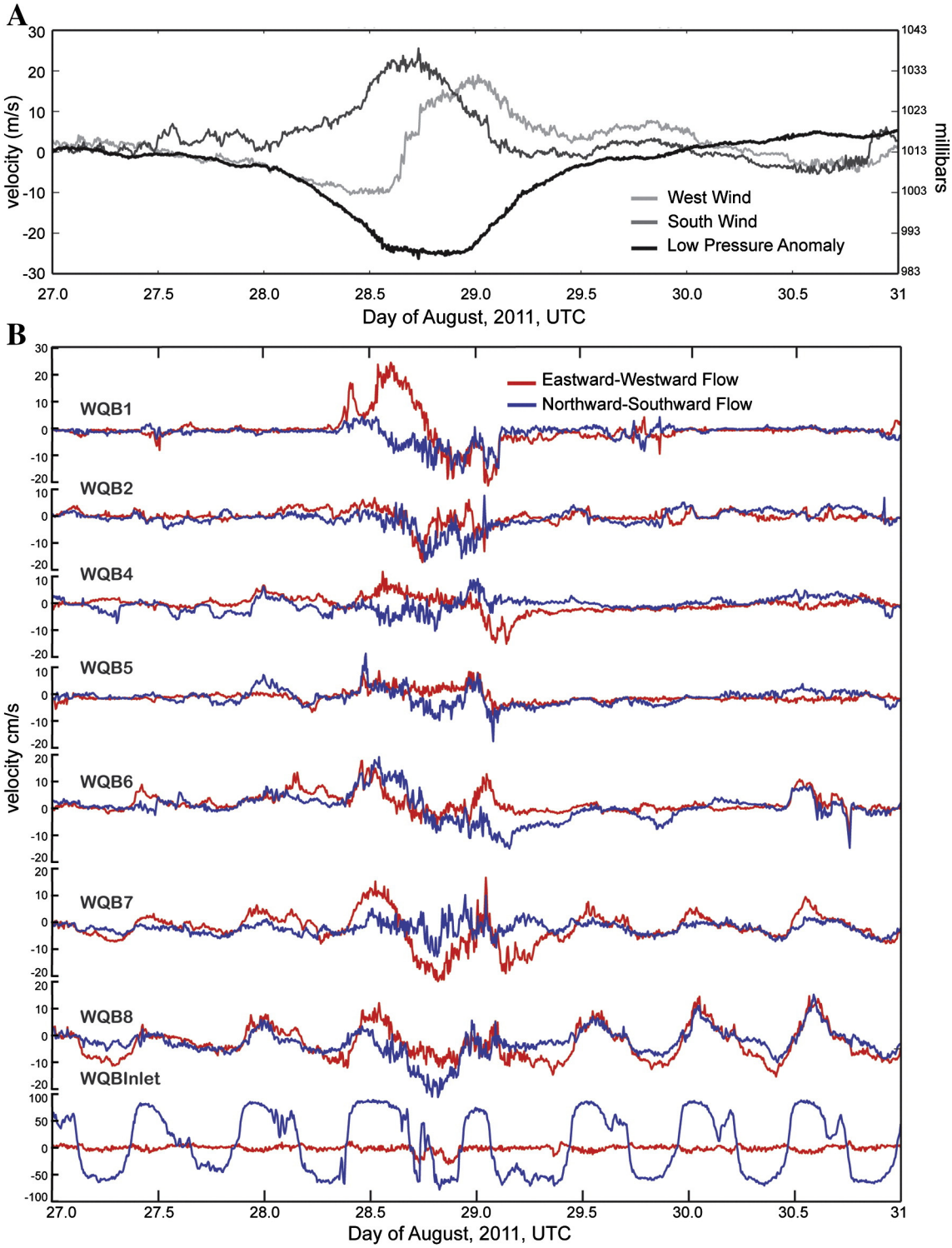

Fig. 4. Wind velocity, air pressure, and current velocity measured during Tropical Storm Irene. A) The south and west components of wind velocities and pressure anomaly from the meteorological station at Menauhant Yacht Club are shown with low pressure (989 mbar) and maximum winds corresponding to peak current flows shown in below plots. B) The summary of near bottom velocities measured by the array of nine current meters. The eastward (positive values) and westward (negative values) components are shown in red while the northward (positive values) and southward (negative values) components are in blue. The scales for individual meters are shown on left. The highest curve corresponds to the 1st site (WQB1) located in the Northern basin, whereas the lowest curve corresponds to the southernmost site (WQBInlet). The WQB3 meter was damaged during the peak of the storm and failed to record data after that point. (For interpretation of the references to color in this figure legend, the reader is referred to the web version of this article.)

of the three cores show that sediments within Unit A have a lower density than those deposited directly below. Unit B comprises the dominant facies within the three cores and is composed of dark grayish-brown sandy mud interspersed with abundant bivalve and gastropod macrofossils. Within WAQ1, this facies is continuous between 40 cm and 600 cm, whereas in WAQ2 and WAQ3, Unit B reaches the depth of 775 cm and 784 cm, respectively. A sub-facies within Unit B consists of well-rounded medium to coarse sand mixed with finer organic rich silts. The sand horizons range from 0.5 cm to 3 cm in width and were difficult to visually discern but showed up readily in radiographs. Unit

Table 2
SLOSH model results for storm surge heights at Woods Hole (WH) and Waquoit Bay (WB). All values are shown in meters relative to MHHW. Bolded values show the storm tide within Waquoit Bay taking into account both the height of the modeled surge and tide coincident with peak surge.

Year	Storm	Peak storm (UTC)	WH tide Gauge (MHHW)	WH tide Correction (MHHW)	WH surge Observed (MHHW)	WH SLOSH (m)	WB SLOSH (m)	WB tide Correction (MHHW)	Storm Radius (km)
2011	Irene	Aug 28, 1300	0.495	−0.365	0.86	0.79	**0.73**	0.365	113
1991	Bob	Aug 19, 1900	1.396	−0.233	1.629	1.77	**1.62**	1.387	46
1985	Gloria	Sep 27, 1900	0.719	−0.603	1.322	1.37	**1.07**	0.467	51
1976	Belle	Aug 10, 0800	−0.299	−0.654	0.355	0.3	**0.27**	−0.384	48
1960	Donna	Sep 12, 2200	1.061	−0.204	1.265	1.25	**0.98**	0.776	35
1954	Carol	Aug 31, 1400	2.54	−0.008	2.548	1.71	**1.46**	1.452	61
1938	Great NE	Sep 21, 2200	2.66	0.032	2.628	2.47	**1.86**	1.892	56
1815	Great Sept	Sep 23, 1700	N/A	−0.058		2.65	**2.04**	1.982	51
1635	Great Col.	Aug 25, 1100	N/A	N/A	N/A	3.72	**2.9**	N/A	56

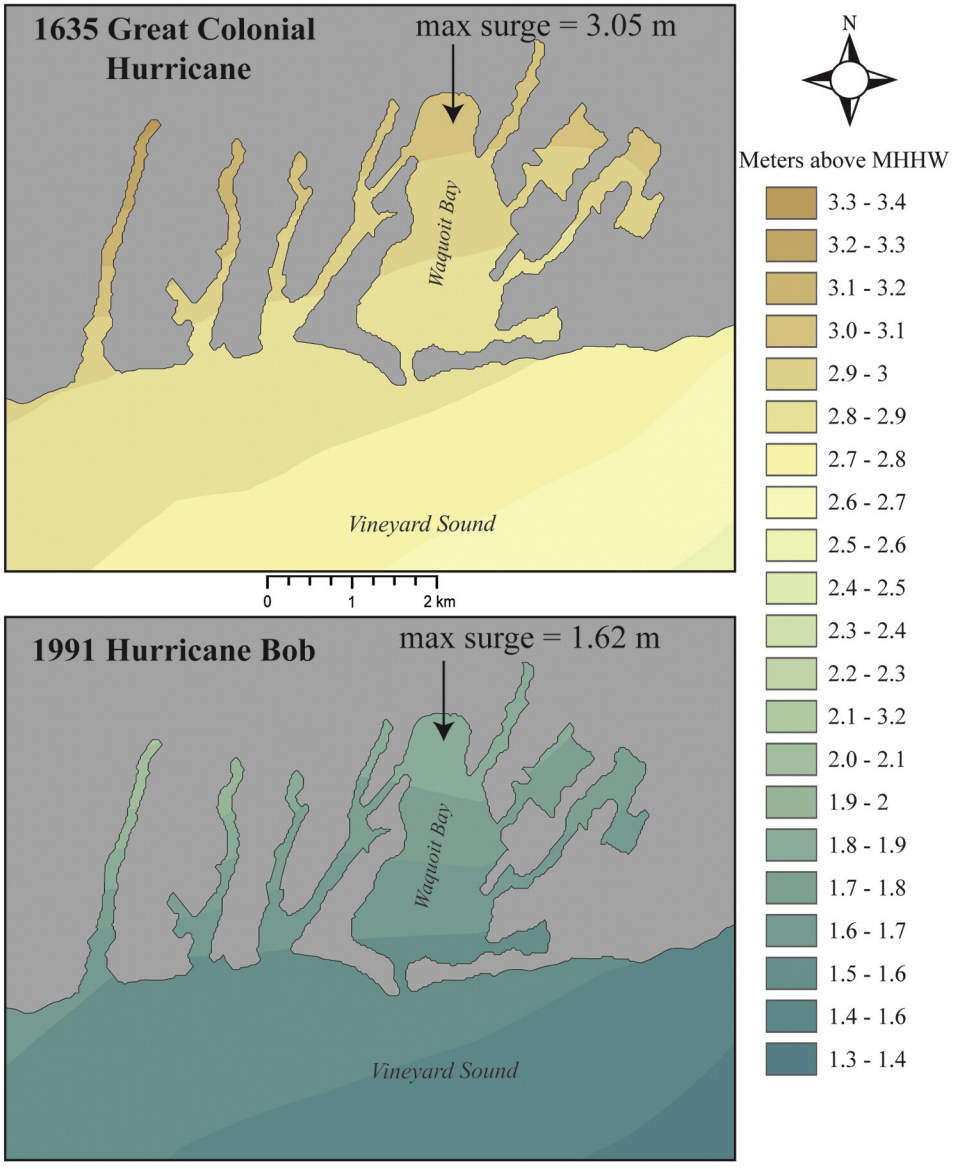

Fig. 5. Modeled storm surge above mean high high water (MHHW) within Waquoit Bay for the Great Colonial Hurricane of 1635 and the 1991 Hurricane Bob. Map colors correspond to the key on the right with dark brown being the highest surge and dark blue being the lowest. The 1635 hurricane is estimated to be the largest storm since records have been kept. Hurricane Bob was the most recent hurricane to cause a significant storm surge within Waquoit Bay. Note the increased height of modeled surge within the north basin, a condition verified by water level meters. Surge heights in this figure have not been corrected for tides. (For interpretation of the references to color in this figure legend, the reader is referred to the web version of this article.)

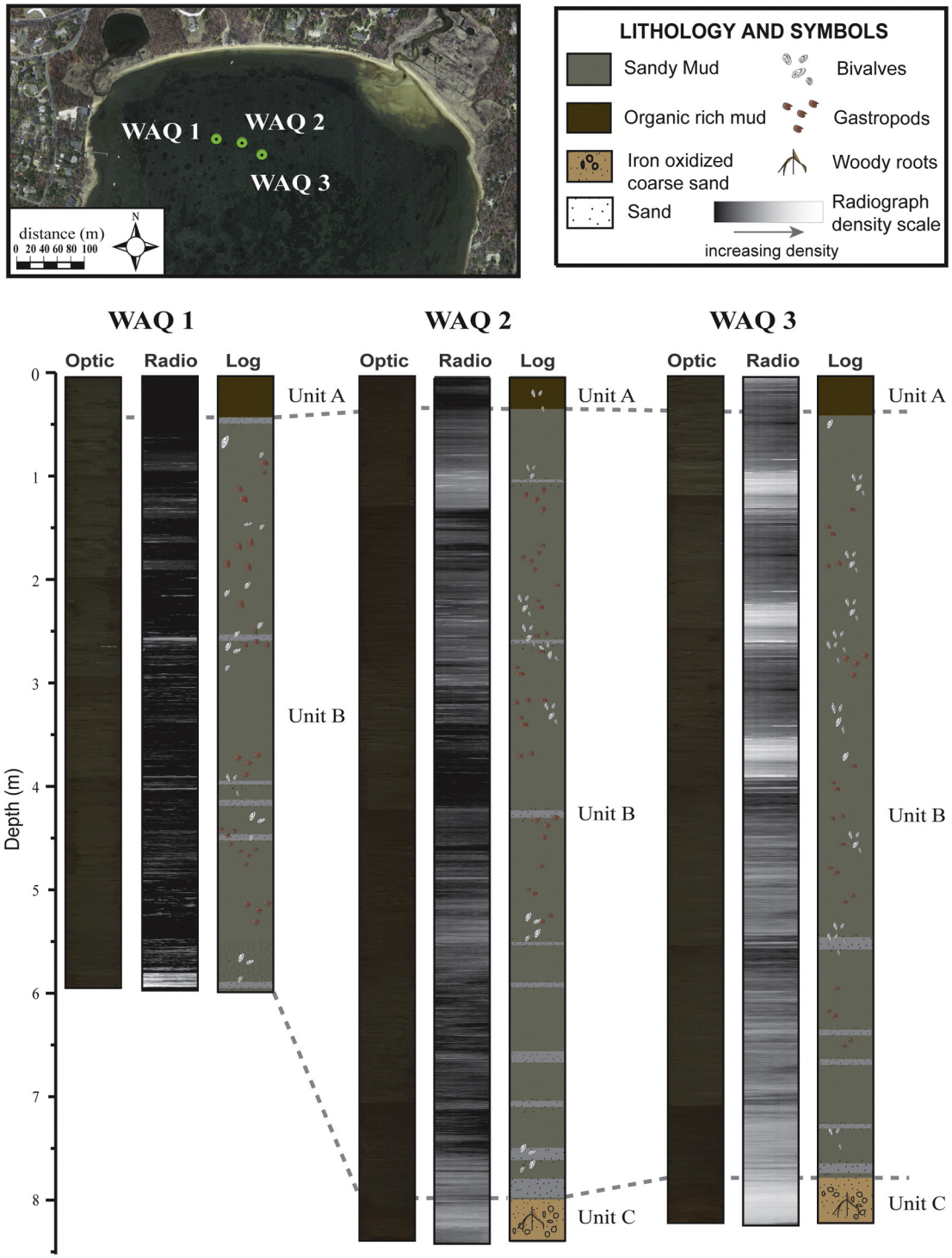

Fig. 6. Optical images, XRF-derived radiographs, and core logs of the three cores. Core locations are shown on the upper insert map and symbology is in the upper right legend. Core stratigraphy has been generally divided into three units (A–C) based on the sediments physical characteristics. Radiographs are shown with white colors signifying increased sediment density and black signifying less dense sediment. The numerous white bands across the three cores indicate an increase in sediment density due to the presence of coarse grain sand, carbonate macrofossils, or a combination of the two. (For interpretation of the references to color in this figure, the reader is referred to the web version of this article.)

C consists of a continuous bed of very coarse sand interspersed with wood fragments, and based on the radiograph, is much denser than the overlying beds. This bed is absent of the finer sediments that dominate the upper portion of the cores. The lower bed is also unlike the coarse grain horizons observed in Unit B as the sand is coarser, angular and poorly sorted, and has a reddish color indicating iron oxidation.

3.4. Grain size analysis

Grain size data reveal highly variable sediment sizes with the dominant fine (<150 μm) sediments being punctuated by thin horizons of larger (>600 μm) sediments (Fig. 7). The mean grain size between the three cores was 155 μm, 155 μm, and 167 μm in WAQ 1, 2, and 3

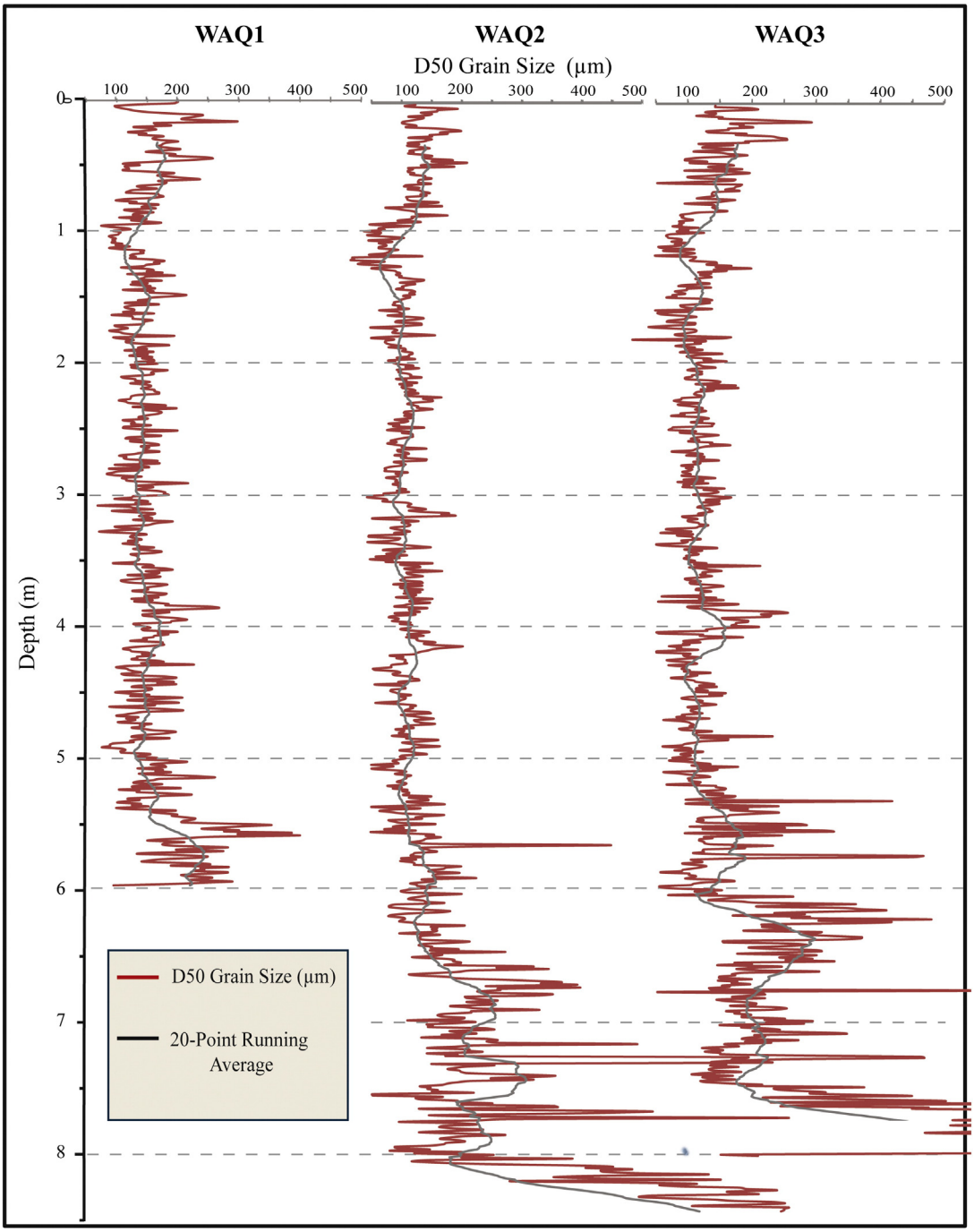

Fig. 7. D50 (median) grainsize data for the three Waquoit cores shown in red. The depth in meters is shown on the left axis with horizontal dashed gray lines corresponding to meter increments. Twenty point running average of mean grain size data is shown with the solid black line and illuminates long term trends. (For interpretation of the references to color in this figure legend, the reader is referred to the web version of this article.)

respectively. The remainder of grain size statistics will be reported using the D90 statistic, which is conducive towards identifying coarse grain anomalies characteristic of high energy sediment transportation events (Boldt et al., 2010). The 20-point running average of D90 grain sizes between the three cores shows considerable similarities in grain size trends with depth (Fig. 8). For example, a distinct decrease in mean sediment size was observed across the three cores between 90 cm −140 cm while a steady increase in sediment size was observed below 5.5 m. Based on the combined hydrographic and sedimentary data coarse grain anomalies within the cores are at least in part related to storm passage.

3.5. Radioisotope data

Although samples for ^{137}Cs and ^{210}Pb dating were collected and analyzed within the gamma detector, the results were inconclusive and we were unable to utilize the information within the age model. ^{210}Pb activity does not go asymptotic at lower depths, possibly indicating disturbance in the sediments. Additionally, the ^{137}Cs data did not have well-defined spikes in activity characteristic of deposition resulting from the onset of atmospheric nuclear weapons testing beginning 1954 followed by a second and larger peak in 1963 (Donnelly et al., 2001). The discrepancies in the data are likely attributed to both natural

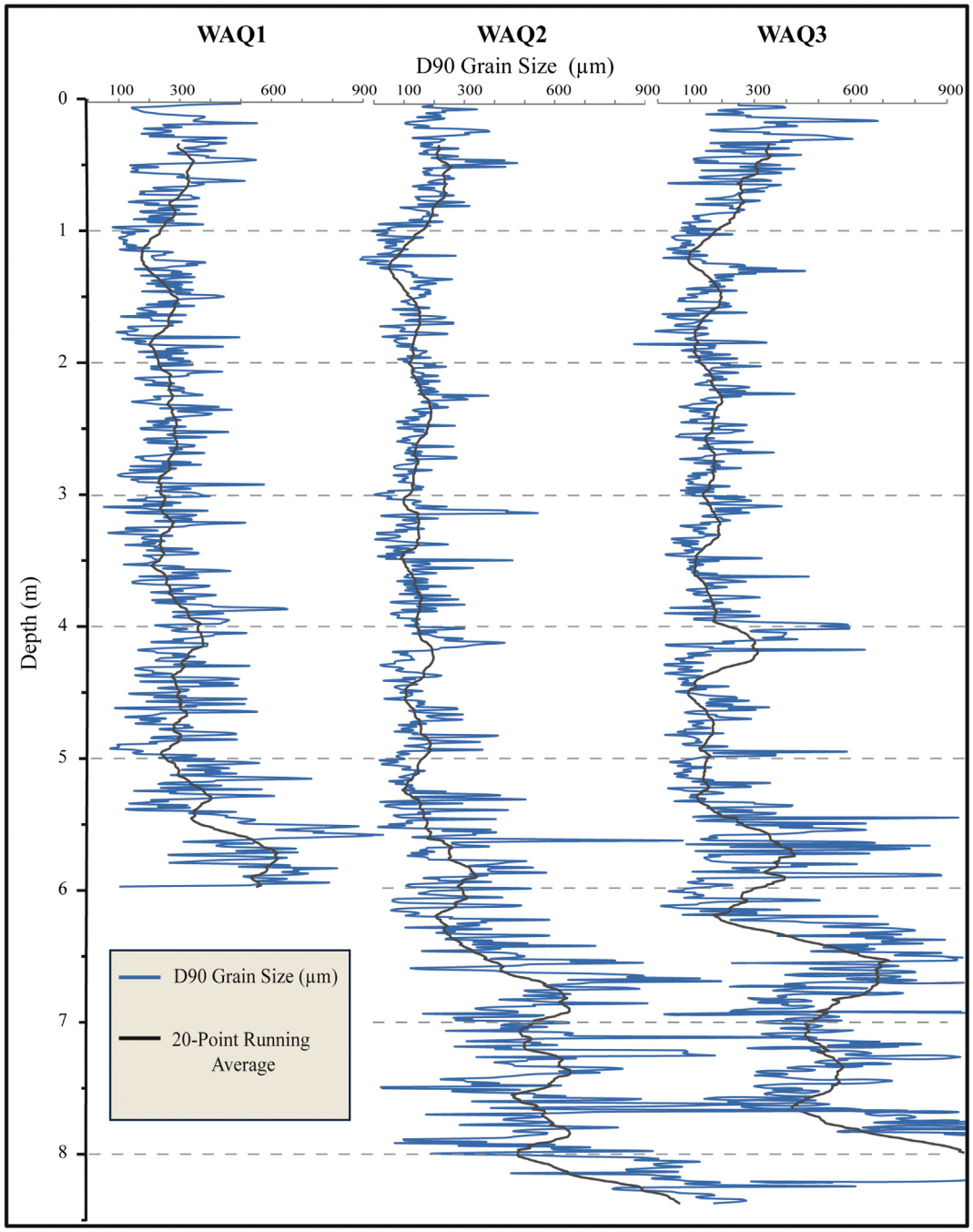

Fig. 8. D90 grain size data for the three Waquoit cores shown in blue. It is assumed that increased D90 values is synonymous with increased energy within the system. The depth in meters is shown on the left axis with horizontal dashed gray lines corresponding to meter increments. Twenty point running average of D90 grain size data is shown with the solid black line and illuminates long term trends. (For interpretation of the references to color in this figure legend, the reader is referred to the web version of this article.)

(groundwater seepage and bioturbation) and anthropogenic (recreational activities) disturbances in the upper sediments. Our inability to utilize these well constrained chronomarkers makes us dependent on the XRF-derived bulk Pb data to determine the age depth model for the past century.

3.6. Radiocarbon

Twenty nine macrofossil bivalves and gastropods were sampled from WAQ1 and WAQ2 and aged using CFAMS methods (Table 3). Dates span the period between 146 ± 145 cal BP (70 cm WAQ1) and 3637 ± 170 cal BP (571 cm WAQ1). Of the 29 dated samples, 8 dates (outliers) do not follow a well-defined age depth relationship, likely indicating the reworking and redeposition of shell material during the historical period. These dates were not included in the age model developed for WAQ1 and WAQ2. The results attest to the considerable uncertainties that arise from applying the CFAMS methods coupled with the assignment of a marine reservoir correction. These combined factors resulted in uncertainties in the calibrated dates between ±90 and ±263 years.

3.7. Bulk lead (Pb) data

We assume that the averaged Pb concentrations below 3 m in the WAQ1 core (156 ints) represents the natural background Pb component within the Waquoit sediments and that an increase in concentrations

Table 3
Radiocarbon dates obtained from aging carbonate shell samples using continuous flow atomic mass spectrometry (CFAMS). All ages were calibrated using Calib version 7.0.1 with the Marine13 calibration data set (Reimer et al., 2013) applying a marine reservoir correction (ΔR) of ΔR = −95 ±45 ^{14}C years (Stuiver and Braziunas, 1993; Little, 1999). Values are reported in calibrated years before present (cal BP) and calibrated years CE/BCE (CE or BCE) within a 1-sigma range. Bolded values indicate the median cal BP and CE/BCE age.

Lab no.	Sample no.	Core	Depth (cm)	^{14}C age	cal CE median	cal CE median (±yrs)	cal BP median	cal BP median (±yrs)	Material dated
113855*	WAQ1_1:6_26	WAQ1 1:6	26	977 ± 168	**1468**	152	**483**	152	Bivalve
113856*	WAQ1_1:6_43	WAQ1 1:6	43	684 ± 167	**1770**	180	**181**	180	Bivalve
107851*	WAQ1_1:6_66	WAQ1 1:6	70	469 ± 96	**1773**	114	**146**	145	Bivalve
107852*	WAQ1_1:6_84	WAQ1 1:6	78	719 ± 97	**1528**	94	**422**	94	Gastropod
109731*	WAQ1_2:6_131	WAQ1 2:6	131	674 ± 152	**1556**	141	**395**	141	Gastropod
106547*	WAQ2_2:6_158	WAQ2 2:6	158	1080 ± 90	**1200**	117	**750**	117	Bivalve
109730*	WAQ1_2:6_190	WAQ1 2:6	190	737 ± 152	**1520**	136	**443**	149	Bivalve
106545*	WAQ2_2:6_75	WAQ2 2:6	195	965 ± 90	**1333**	82	**618**	82	Bivalve
111455*	WAQ2_3:6_42	WAQ2 3:6	213	1345 ± 127	**942**	146	**1009**	146	Bivalve
109741	WAQ1_3:6_24	WAQ1 3:6	217	799 ± 262	**1458**	238	**493**	238	Bivalve
113857	WAQ1_3:6_240	WAQ1 3:6	240	1310 ± 167	**1172**	156	**778**	156	Bivalve
109740	WAQ1_3:6_79	WAQ1 3:6	272	997 ± 262	**1263**	241	**686**	241	Bivalve
113858	WAQ1_4:6_297	WAQ1 4:6	297	1682 ± 170	**828**	174	**1122**	174	Bivalve
113859	WAQ1_4:6_345	WAQ1 4:6	345	1541 ± 168	**954**	179	**996**	179	Bivalve
106546	WAQ2_3:6_79	WAQ2 3:6	345	1360 ± 90	**935**	109	**1015**	109	Bivalve
113860	WAQ1_4:6_363	WAQ1 4:6	363	1921 ± 169	**556**	188	**1395**	188	Bivalve
109742	WAQ1_4:6_88	WAQ1 4:6	380	1338 ± 262	**965**	254	**985**	254	Gastropod
111454	WAQ2_3:6_111	WAQ2 3:6	382	1534 ± 126	**778**	135	**1173**	135	Bivalve
106544	WAQ2_4:6_409	WAQ2 4:6	409	1640 ± 90	**670**	103	**1280**	103	Bivalve
109747	WAQ1_5:6_34	WAQ1 5:6	426	1753 ± 262	**529**	290	**1421**	290	Gastropod
111452	WAQ2_4:6_132	WAQ2 4:6	447	2361 ± 127	**−173**	164	**2122**	164	Bivalve
109749	WAQ1_5:6_64	WAQ1 5:6	456	1971 ± 263	**313**	299	**1638**	299	Bivalve
109748	WAQ1_5:6_77	WAQ1 5:6	469	2404 ± 262	**−205**	330	**2155**	330	Gastropod
111451	WAQ2_5:6_90	WAQ2 5:6	550	2910 ± 129	**−598**	162	**2547**	162	Bivalve
111445	WAQ1_6:6_99	WAQ1 6:6	571	3615 ± 128	**−1688**	170	**3637**	170	Bivalve
111446	WAQ1_6:6_84	WAQ1 6:6	576	3351 ± 129	**−1364**	174	**3312**	173	Bivalve
113861	WAQ1_6:6_592	WAQ1 6:6	592	3385 ± 236	**−1162**	285	**3111**	285	Bivalve
111449	WAQ2_6:6_2	WAQ2 6:6	607	3306 ± 127	**−1311**	170	**3255**	175	Gastropod
111450	WAQ2_6:6_52	WAQ2 6:6	757	3577 ± 128	**−1640**	169	**3589**	169	Bivalve

Asterisks indicate samples were not included within the age model due to the possibility of reworked material and uncertainties associated with radiocarbon ages during the historic period.

above these background levels represents introduction from anthropogenic sources (USEPA, 2000; Lima et al., 2005; Kemp et al., 2012). Within the Waquoit sediments, an initial increase in Pb above background levels is first observed at 120 cm (WAQ1), and 138 cm (WAQ2). (Fig. 9). Pb levels do not again decrease to near background levels until the upper 10 cm of sediments. A maximum Pb levels within the WAQ1, and WAQ2 was recorded in the sediments at 73 cm (562 ints), and 76 cm (483 ints) respectively.

The earliest Pb chronomarker can be identified within sediments by the steep increase in Pb concentrations above background levels as a result of the Industrial Revolution (Lima et al., 2005; Kemp et al., 2012). This is recorded at 109 cm within WAQ1 and 130 cm in WAQ2 and assigned a date of 1875 ± 6 CE (Nriagu, 1998; Lima et al., 2005; Kemp et al., 2012). A peak in the consumption of leaded gas has been documented to have occurred in 1974 (USEPA, 2000), which was recorded at 32 cm within both cores. The phase out of leaded gas after the 1970 Clean Air Act resulted in a rapid fall in Pb emissions, and by the mid 1980s concentrations had almost returned to background levels (250 ints) (USEPA, 2000) This is recorded at 19 cm in WAQ1 and 25 cm in WAQ2 and assigned the year of 1986 ± 6 CE.

4. Discussion

Interpreting the results will aid in deciphering the Waquoit sedimentary record and its response to storm passage. The results presented indicate that passing storms have a significant impact on sediment dynamics within the lagoon by rapidly altering transport pathways and depositional patterns. These dynamics have left a pattern of coarse sand horizons deposited during high amplitude low frequency events interbedded with fine organic rich estuarine sediments (Fig. 6 - Unit B). During the passage of Irene, high velocity water currents moving at various depths and directions were capable of eroding and transporting sand from several landward and seaward sources ultimately resulting in the deposition of a sand layer within the north basin observed in the WAQ2 and WAQ3 cores. Irene provides a modern analogue for a storm-induced mechanism for depositing sand at the coring site.

4.1. Core stratigraphy interpretation

Based on grain size, physical description, and density, we infer Unit A represents unconsolidated modern estuarine sediments not yet compacted by overlying beds (Fig. 6). The gelatinous composition of Unit A may be attributed to it having a rich organic content resulting from the modern proliferation and decomposition of algal species characteristic of eutrophication within the groundwater fed estuaries of Cape Cod (Bowen and Valiela, 2001; Fox et al., 2012). Unit B represents an estuarine facies made up of organic rich fine sediments mixed with fine to medium sand. Grain size analysis revealed that these finer sediments are punctuated by coarse sand horizons that are a proxy for high energy conditions characteristic of storm events. A radiocarbon age of 3589 ± 169 cal BP obtained from an articulated bivalve sampled at the bottom of WAQ2 Unit B (757 cm), marks the lowermost depth that can be correlated to estuarine deposition.

Because the bivalve species at 757 cm is the same species identified in modern sediments, we infer that the coring location has remained protected behind a coastal barrier and that during the past 3500 years estuarine conditions have not changed significantly at the coring site. This is corroborated by sea-level records that show that after 6000 ybp, the rate of SLR began to stabilize and coastal and aeolian processes played a larger role in modifying the shoreline forming the coastal features most associated with Cape Cod, including barrier beaches, dunes, saltmarshes, and spits (Fairbanks, 1989; Uchupi and Mulligan, 2006). Based on pollen analysis, the Waquoit marshes transitioned from fresh to brackish systems approximately 4000 ybp, an event that is likely closely related to the marine transgression and establishment of estuarine condition (Orson and Howes, 1992; Maio et al., 2014). Since 1920, there has been a threefold increase in the rate of SLR, when compared with the previous millennium from 1 mm/yr to 3 mm/yr, resulting in widespread landward migration of coastal

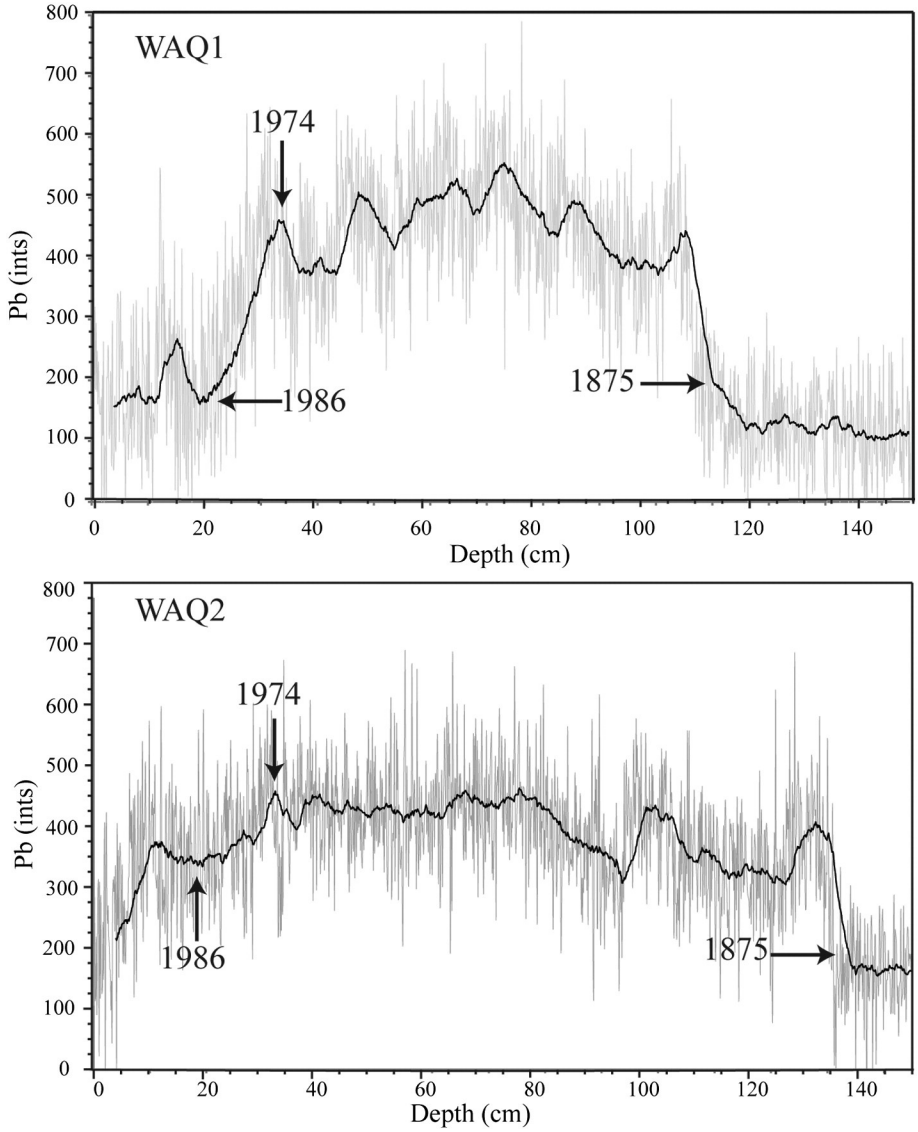

Fig. 9. XRF derived bulk Pb concentrations for the upper 145 cm of WAQ 1 and WAQ2. The typical bell shaped pattern of pollution derived Pb concentrations, where there is an initial increase from background levels, a series of peaks and troughs, and ending with a subsequent drop back to near background levels in the upper sediments, is observed within WAQ1 and WAQ2. The three Pb pollution chronomarkers are identified with the arrows (1986, 1974, and 1875).

landscapes (Donnelly, 2005; Kemp et al., 2009; Maio et al., 2012; Gontz et al., 2013).

Within Unit B, between 5.9 m (WAQ1) and 6.2 m (WAQ2 and WAQ3), there is an unprecedented increase in grain size. Between 1 cm and 6 m within WAQ2 there is a mean D90 grain size of 262 μm, whereas between 6 m and 8.4 m the mean is 669 μm representing a 225% increase. There are several plausible explanations for the down core increase in grain size including, morphological changes, increased energy in the system, and the reworking of abundant outwash sands.

Based on the sediments' physical characteristics, we infer that Unit C likely represents a subaerially exposed terrestrial environment characteristic of an outwash plain. Outwash sand can be observed eroding from the bluffs surrounding the north basin. The Mashpee Pitted Outwash Plain underlies the entire Waquoit system and its presence at these depths can be expected (Orson and Howes, 1992; Rosen, 2003; Maio et al., 2014). Unit C consists of coarse sediment and woody root matter, with a paucity of fine sediments and marine macrofossils found in Units A and B. The absence of a facies representing a fresh water aquatic environment within the cores suggests that unlike some of the native salt marshes (i.e. Orson and Howes, 1992), the north basin may not have evolved from a freshwater to marine environment as sea levels rose, but rather transitioned rapidly from a terrestrial environment to a protected estuary. Alternatively, the absence of a freshwater lacustrine or marsh facies could also be attributed to an erosional unconformity resulting from a high energy event directly preceding the establishment of estuarine conditions.

4.2. Calculation of sedimentation rates

Developing an accurate age model is a key component to determining whether there is a relationship between coarse grain anomalies in the modern and historical sediments and documented storm events. It is also critical to accurately calculate storm frequency as you need to know how many centimeters equals a given number of years. For example, to determine the number of storms per century we need to determine how many centimeters represent that particular century of time and then count the positive anomalies within that interval. This is made more difficult when sedimentation rates are non-linear through time as is the case in Waquoit. A Bayesian age model was developed for WAQ1 and WAQ2 based on the XRF-derived Pb data and ^{14}C dates for the pre-18th century period. Ages were calculated with 95%

Confidence Intervals and are reported as median cal yr. BP (cal BP) or median cal yr. AD (AD).

Positive coarse grain anomalies were plotted with the corresponding age model for WAQ1 and WAQ2 cores (Figs. 10 and 11). Accumulation rates were relatively similar with an average long term rate in both cores of 3.5 mm/yr. In both cores rates of accumulation were markedly higher within the upper 1 m of sediments with maximum rates of 10 mm/yr near the surface. For example, within the upper 1 m of WAQ1 there was a mean sedimentation rate of 7.6 mm/yr while the mean rate for sediments falling below the upper meter was 2.7 mm/

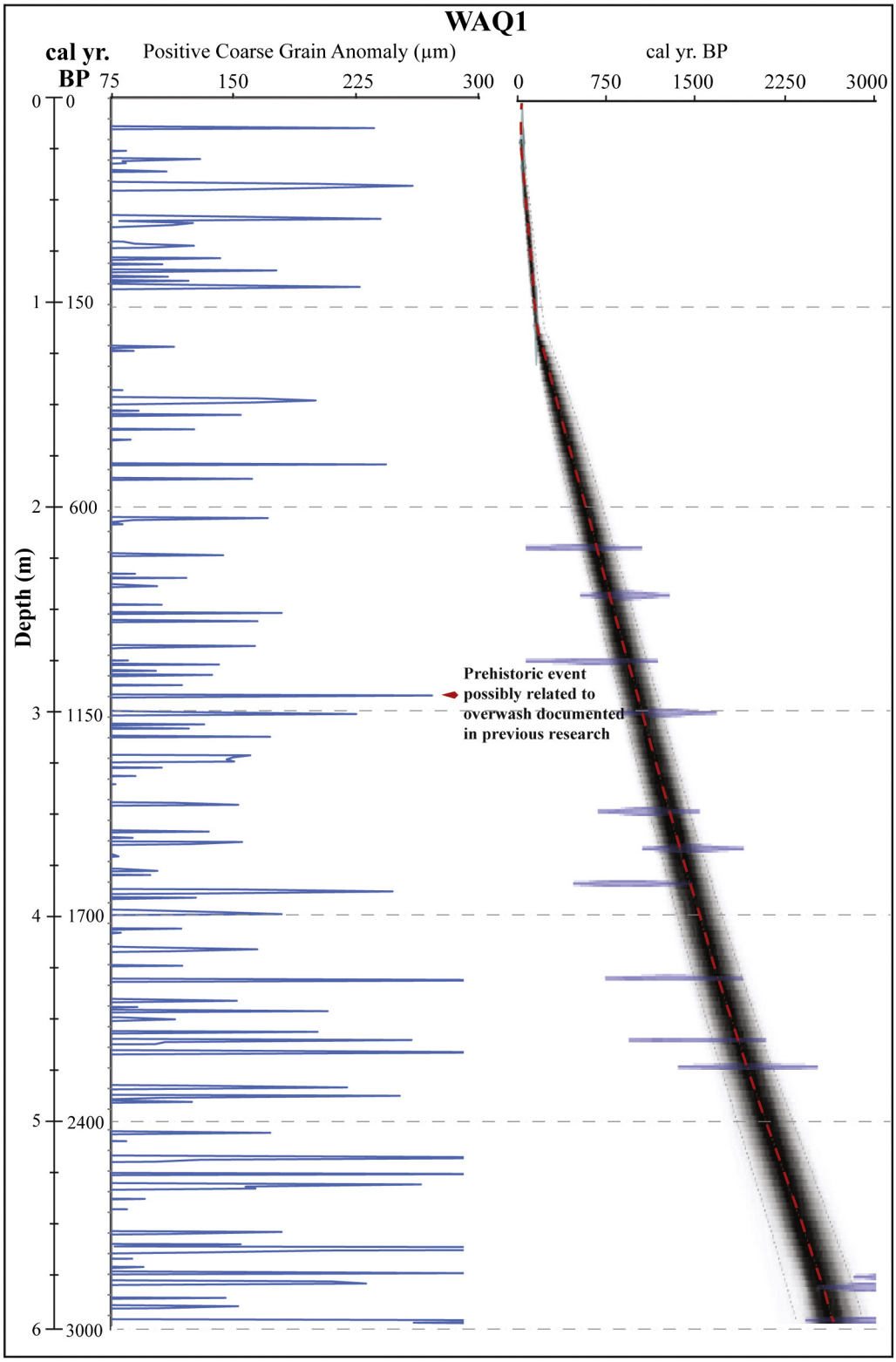

Fig. 10. Positive coarse grain anomalies identified in WAQ1 with corresponding age model. The dashed red line within the plotted age model depicts the median age while the gray scale area shows the 95% confidence interval envelope. Horizontal error bars shown for the bulk lead chronomarkers and CFAMS radiocarbon ages. Note the well constrained model in the upper meter and the increasing uncertainty envelope with depth. The red diamond identifies an anomaly that may correlate to a large storm event documented in other regional studies (e.g. Orson and Howes, 1992). (For interpretation of the references to color in this figure legend, the reader is referred to the web version of this article.)

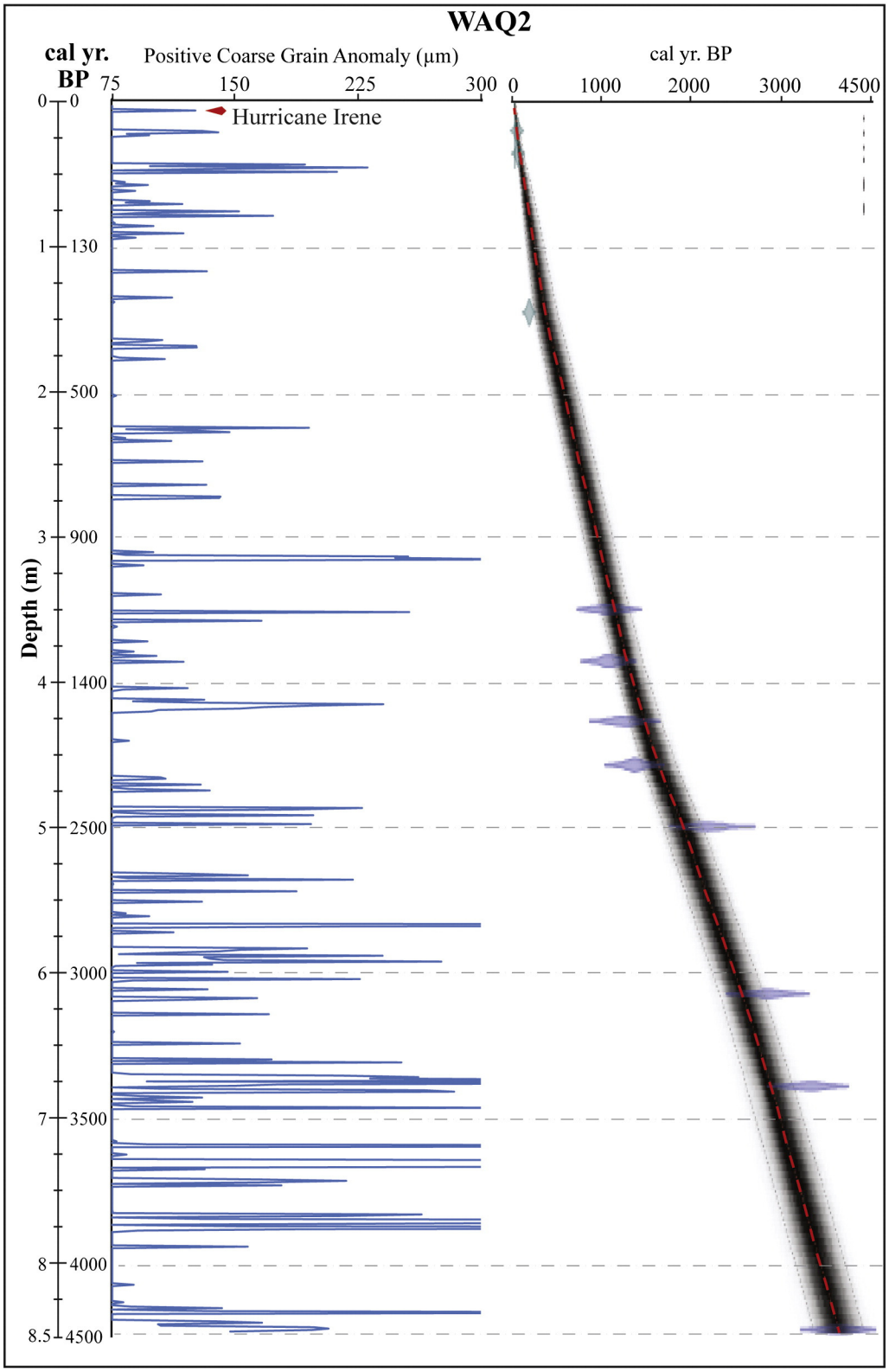

Fig. 11. Positive coarse grain anomalies identified in WAQ2 with corresponding age model. The dashed red line within the plotted age model depicts the median age while the gray scale area shows the 95% confidence interval envelope. Horizontal error bars shown for the bulk lead chronomarkers and CFAMS radiocarbon ages. The positive anomaly near the surface (red diamond) is assumed to be deposited as a result of Irene. (For interpretation of the references to color in this figure legend, the reader is referred to the web version of this article.)

yr. The 95% Confidence Interval for the age model significantly increases with depth with an envelope of ± 10 years in the upper 30 cm increasing to as high as ± 300 years below 5 m. This is primarily due to the age model being based on the more tightly constrained Pb chronomarkers in the upper sediments and a limited number of CFAMS ages with considerable uncertainties deeper in the core.

The data indicates there was a substantial increase in sedimentation rates during the mid to late 18th century. The increase in sedimentation

rates during the historical period is likely closely tied to the combined impacts of human modifications such as land clearance along the upland areas directly adjacent to the bay, cranberry agriculture, and the enlargement and fortification of the main entrance. Furthermore, rapid coastal development during the past 30 years and an increase in recreational activities likely also contributes to increased accumulation rates.

Previous research has calculated varying accumulation rates for the upper sediments of Waquoit Bay spanning from a ^{210}Pb derived 3.5 mm/yr (French, 2007) to an AMS ^{14}C derived 4.5 mm/yr (Rosen, 2003). Both values are nearly half the rate calculated in this study. These variations in reported accumulation rates are likely due to the combined factors of anthropogenic and natural disturbances in the upper sediments, mobility of ^{137}Cs, and ^{210}Pb radioisotopes due to groundwater leaching, and uncertainties with various dating techniques. There are many natural and anthropogenic mechanisms of disturbance that complicate the stratigraphy in the upper sediments of shallow water estuaries. Within Waquoit Bay, disturbance mechanisms include bioturbation from abundant gastropods and bivalves, groundwater leaching, seawater infiltration, commercial shellfishing, and the presence of a recreational mooring field (French, 2007; Rosen, 2003). The combined disturbances appear to have resulted in the mixing of the upper sediments leading to a discontinuity in the ^{137}Cs and ^{210}Pb data. Furthermore, radioisotopes are significantly more mobile in estuarine sediments when compared to stable heavy metals such as bulk-Pb, making them particularly susceptible to disturbance as was observed in our data (French, 2007). The more stable bulk Pb coupled with previous research documenting pollution chronomarkers in U.S. northeast sediments (e.g. Legra et al., 1998; Kemp et al., 2012) were key components to selecting bulk Pb chronomarkers for Waquoit.

4.3. Mechanisms of sand transport into the north basin

Based on the hydrographic, historical, and sedimentary data it appears that storms play a significant role in producing the sand horizons in the cores. We infer that during storm passage the primary sources of sand entering the north basin are, 1) the upland bluffs and beaches comprising the northern shoreline directly adjacent to the basin, 2) the ebb tide deltas fronting Caleb Pond along the northeastern shoreline and those fronting the eastern and western shorelines southward of the basin, and to a lesser degree, 3) eroded and windblown sand from the barrier itself (Fig. 12). The sand from these sources is inferred to be transported within the water column through both surface and bottom currents. As there is no major fluvial drainage entering directly into the north basin, this was excluded as a possible source of coarse event beds.

The build-up of surging storm waters concurrent with a 25 m/s alongshore current results in the rapid excavation of upland bluffs, erosion of beaches, and removal of shallow shoreface and ebb tide delta sands. Windblown surface waves magnify the energy of the surging water column leading to a strong landward moving surface current (Fig. 12C). Once mobilized within the swash zone, the suspended sediments are transported within alongshore and seaward moving bottom

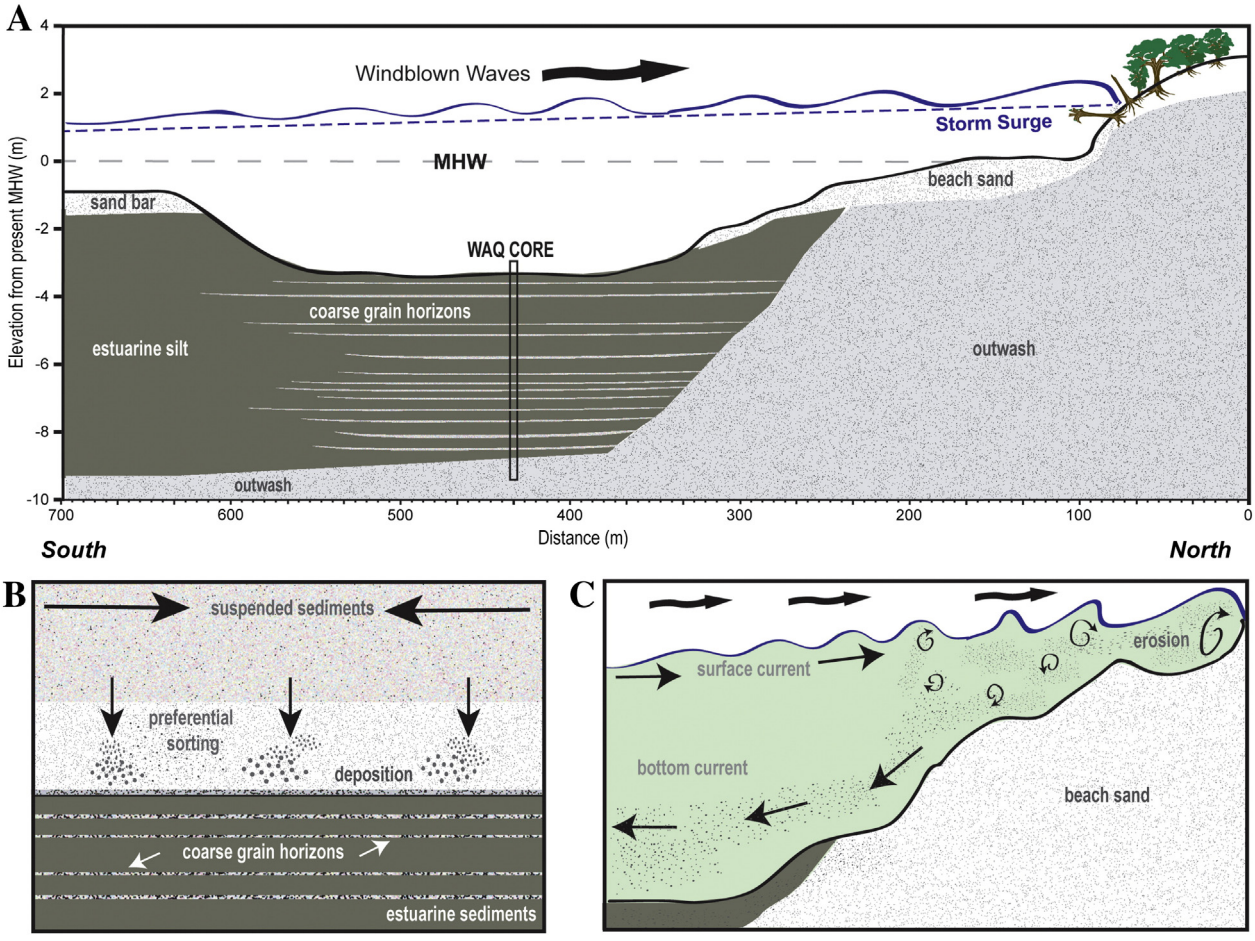

Fig. 12. Conceptual model of mechanisms leading to the formation of coarse grain horizons within the Waquoit cores. A) Conceptualized cross section of the north basin showing core location, outwash, beach, and bar sands. The current MHW is shown with the dashed gray line and a 1 m storm surge is shown with the blue dashed line. Windblown waves further increase the height of the storm tide resulting in excavation of upland bluffs and erosion of beach and shoreface sand. B) Once sand is transported into the north basin it is preferentially sorted and is deposited on the basin floor. C) The build-up of storm surged water within the north basin sets up the conditions for a strong alongshore and offshore bottom currents capable of transporting sand into the basin. (For interpretation of the references to color in this figure legend, the reader is referred to the web version of this article.)

currents. The return flow transports the sediment rich water along an energy and gravitational gradient from the high energy shoreface down into the low energy basin. According to the Hjulstrom (1939) diagram, a water column will erode, transport, or deposit sediment depending on the grain size and flow speed. For example, for medium sand with a grain size of 500 μm, the transport range is from 3 cm/s to 25 cm/s. Based on this relationship, the near bottom return flow of 10 cm/s persisting for 6 h is capable of transporting medium size sand a distance of about 2 km. As was observed during Irene, even during that relatively small storm these conditions resulted in the deposition of a coarse grain event bed within the north basin.

In addition to the sand arriving at the coring site from the landward shoreface, it is also likely that it arrives from seaward locations including the shallow (<1 m) ebb tide deltas extending from the eastern and western shorelines and to a lesser degree from the barrier itself. The current meter located within the main channel into the lagoon (WQBEInlet) recorded a velocity of 75 cm/s, capable of causing significant erosion of adjacent beaches and entraining sand in the landward moving currents. When these currents override the shallow bars additional sand grains are suspended and transported landward into the north basin.

When quantifying the processes that have led to the storm-induced coarse grain anomalies based on the Irene hydrographic data, it is important to note that Irene was downgraded to a tropical storm when it made landfall, over 200 km west of the study site. Because this event was considerably less intense than most of the historical hurricanes impacting Waquoit Bay based on the SLOSH model runs (0.37 m storm tide), but nonetheless left a sedimentary signature of its passage (Fig. 11), we assume the hydrographic data serves as a minimum threshold for storm conditions within Waquoit Bay. Though we don't have any data for hydrographic conditions within Waquoit Bay during extratropical storms, it must be assumed that if they resulted in surges of similar magnitude to Irene, regardless of wind direction, a sand layer would likely be deposited.

4.4. Coarse grain anomalies and storm passage

Deciphering the role storms play in the sediment dynamics of Waquoit Bay and whether a discernable proxy record of past hurricanes is preserved in the sediments is dependent on answering the question of whether the dates assigned (based on the age model) to the positive grain size anomalies correlate to observed storm events impacting the region (Table 1). SLOSH results serve to identify which of these storms were most likely to have resulted in a significant storm surge within the lagoon (Table 2).

Given the fact that the uncertainties in the age-depth model during the historical interval range from ±10 to ±140 years (increasing with depth), it is not possible to precisely correlate individual anomalies to documented storm events. However, discussing how the median year corresponding to a particular anomaly compares to the passage of notable storms is warranted. Using the WAQ1 core, 20 positive coarse grain anomalies were identified in the upper 1.5 m of sediments (1625–2011 ± 65 CE) and then assessed for their relationship to documented storm events (Fig. 13). There does seem to be some correlation between the median age of the largest of the anomalies and the passage of both strong hurricanes and Nor'easters. However, other anomalies do not clearly align with observed storms.

The first positive anomaly within WAQ1 occurs between 14 cm and 17 cm. Given its depth near the surface, observed and modeled storm impacts, and the absence of major storm events between 1991 and 2010, this horizon is likely associated with Hurricane Bob (1991). Bob made landfall 40 km to the west of Waquoit in Newport, RI as a Category 2 storm. The south shores of the upper Cape and Buzzards Bay were hit particularly hard due to their position along the eastern edge of the storm. The observed storm tide at the Woods Hole tide gauge was 1.40 m above MHHW while the SLOSH modeled storm tide within

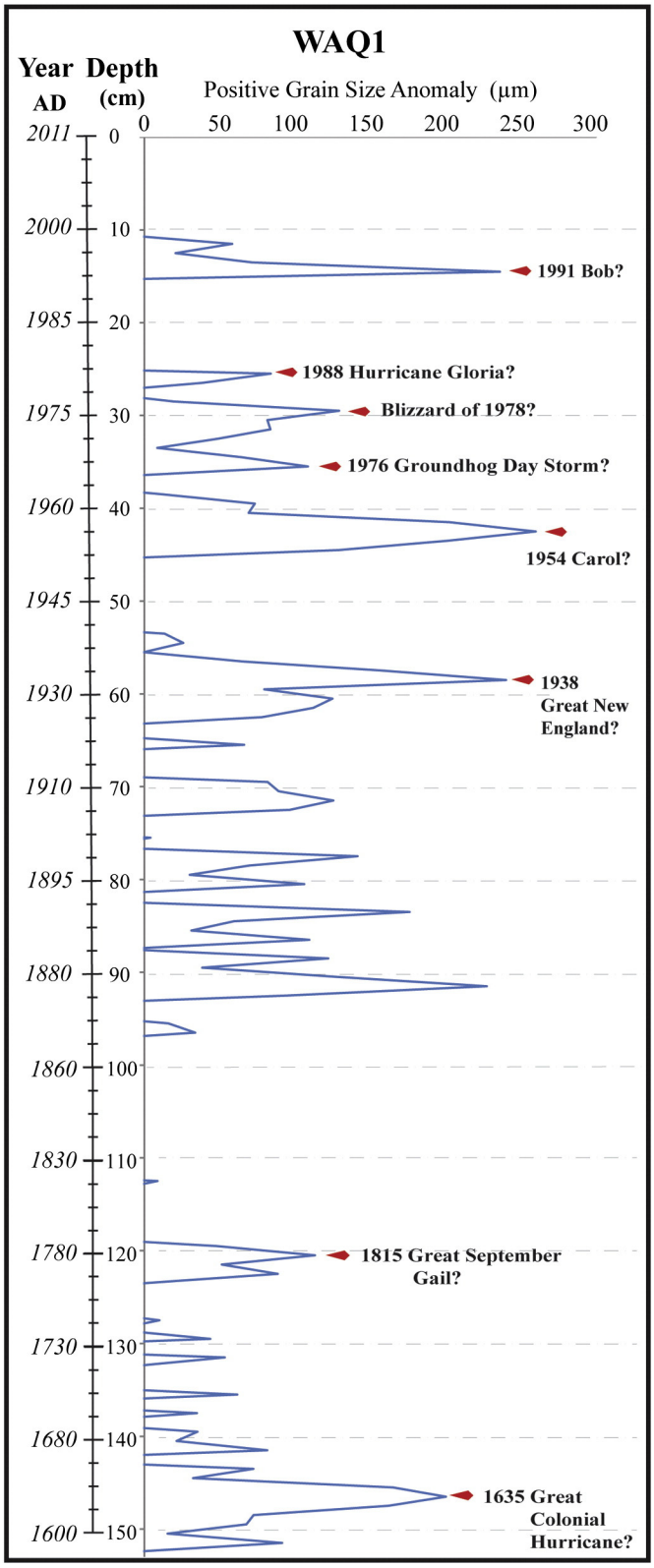

Fig. 13. Coarse grain anomalies identified in the upper 1.5 m of WAQ1 shown with age AD and corresponding depth on left. Documented storm events that may correlate to positive coarse grain anomalies are identified with the red diamond and storm name. Increasing sedimentation rates with depth result in a non-linear age model. (For interpretation of the references to color in this figure legend, the reader is referred to the web version of this article.)

Waquoit Bay was 1.39 m above MHHW (Fig. 5). The storm caused a major breach through the Washburn barrier that, up until then, had separated the Vineyard Sound and Eel Pond, temporarily making Waquoit Bay a three inlet higher energy system (Aubrey et al., 1993; Valiela et al., 1998; National Hurricane Service, 2013). This event was also recorded in nearby Salt Pond (i.e. Donnelly et al., 2015) and Mattapoisett Marsh (i.e. Boldt et al., 2010).

Event beds between 22 cm (1985 ± 12 CE) and 33 cm (1972 ± 15 CE) may correlate to the three major storm events occurring during that time including Hurricane Gloria (1988), The Blizzard of '78 (Nor'easter), and the Groundhog Day Storm of 1976 (Nor'easter). Below this, the largest of the anomalies in the upper sediments corresponds to a date of 1954 ± 30 CE and may be the event bed left from Hurricane Carol (1954), which resulted in widespread devastation to the region and a modeled storm tide of 1.5 m above MHHW within Waquoit Bay. Moving further down the core another large anomaly is centered at 62 cm with a corresponding date of 1932 ± 38 CE. This event bed may be associated with the Great New England Hurricane of 1938, which had a modeled storm tide of 1.9 m. Between 65 cm and 100 cm there is an additional 7 anomalies that do not clearly correlate to documented storm events. Below this, a more quiescent period in the record occurs between 100 cm (1858 ± 70 CE) and 118 cm (1800 ± 94 CE) with only 1 anomaly being recorded.

An anomaly centered at 120 cm (1790 ± 104 CE) may correlate to Great September Gale of 1815, though the increasing uncertainties in the age model make this assignment more speculative. The estimated Category 3 storm was the largest of the 19th century, making landfall along the Connecticut coastline (Boose et al., 2001; Boldt et al., 2010; NHS, 2013). To the west, the southern facing lagoons of Rhode Island and Massachusetts took the brunt of the storm surge as peak wind speeds came coincident with high tide (Ludlum, 1963). A report from Narragansett Bay indicates storm surges exceeding 3 m, "wind brought in the tide ten or twelve feet above the height of the usual spring tides, and seven and a half feet higher than ever known before" (Ludlum, 1963). In addition to these historical accounts, SLOSH model outputs put the storm tide in Waquoit Bay at 2 m, making it the second largest of the modeled surges.

A series of smaller anomalies is proceeded by the earliest recorded during the historical time period centered at 146 cm (the 1641 ± 140 CE). This event bed may be associated with the Great Colonial Hurricane of 1635, which resulted in storm surges within Buzzards Bay exceeding 6 m (Ludlum, 1963; Boose et al., 2001; Boldt et al., 2010). The severity of this event and the SLOSH results make it likely a signature of its passage was archived in the Waquoit sediments. The devastation resulting from the 1635 hurricane was said to not to be seen again until the September Gail of 1815, 180 years later (Ludlum, 1963). A report from John Winthrop, then Governor of the Massachusetts Bay Colony, states; "The tide rose at Narragansett fourteen feet higher than ordinary, and drowned eight Indians flying from their wigwams" (Ludlum, 1963). These historical reports are validated by SLOSH results, which modeled a 3.1 m storm tide above MHHW within Waquoit Bay (Fig. 5).

Given the increasing uncertainties in the prehistoric sediments (±140 to ±300 years) it is not possible to delineate a set period of time (century) in which to count anomalies within, and, thus, event frequency cannot be calculated. However, some of the larger event beds in the prehistoric sediments may be related to storm-induced environmental changes documented in previous research including a storm event(s) occurring between 1100 and 1200 CE (e.g. Orson and Howes, 1992; Buynevich and Donnelly, 2006; Madsen et al., 2009; Maio et al., 2014). Based on our age model, the largest anomaly in the upper 4 m of WAQ1 occurs at 292 cm (1168 ± 188 CE) and appears to correlate with large overwash deposits identified within the Sage Lot Pond marsh sediments dated to ~1100 CE, which led to wide scale shifts in native plant communities (Orson and Howes, 1992). This event bed could also relate to an overwash layer identified within Little Sippewissett Marsh, located 10 km west of Waquoit Bay, dating to between 994 CE and 1149 CE, while at Mattapoisett Marsh, three events were recorded during the same period (Buynevich and Donnelly, 2006; Boldt et al., 2010).

4.5. Limitations of site for use in storm reconstruction

Our interpretation of the data presented indicates that the sediment dynamics of Waquoit Bay are heavily impacted by weak and strong storms with both tropical and extratropical origins. During storm passage the increase in surface and bottom currents leads to environmental conditions favoring the transport of coarse sediments into the north basin in both landward and seaward directions. However, due to variable sediment sources and transport pathways, the sensitivity of the site to both tropical and extratropical storms, and the uncertainties with the age model there is little utility in calculating long-term hurricane frequencies at this time. Discussing some of the reasons behind why we're unable to calculate accurate frequencies is beneficial to future site selections.

The primary mechanisms of deposition (seaward moving bottom current) identified in this study is in contrast to previous paleotempestological studies where storm-induced horizons are inferred to be derived from barrier sand transported through newly formed breachways or directly by overwash being deposited within adjacent back-barrier saltmarshes (e.g. Donnelly et al., 2001; Scileppi and Donnelly, 2007; Boldt et al., 2010), or salt ponds (e.g. Emery, 1969; Liu and Fearn, 2000; Brandon et al., 2014; Donnelly et al., 2015). The differences between sediment transport processes leading to event bed chronologies in previous studies and that of those occurring within Waquoit Bay may account for the challenges in differentiating between tropical and extratropical events and calculating an accurate number of hurricanes per century.

The sensitivity of Waquoit Bay also is a factor. In contrast to the 20 coarse grain anomalies identified in the Waquoit sediments during the instrumental period, only the two largest hurricanes during the 20th century left a sedimentary signature in Succotash Marsh, including Carol (1954) and the Great New England Hurricane (1938). Within Salt Pond, 6 km - west of Waquoit Bay, only 3 events were recorded during the historical record including hurricanes in 1991, 1675, and 1635 (Donnelly et al., 2015). This indicates that at least during the historical interval Waquoit Bay has been more sensitive to storm events than these other locations.

Differences in the number of event beds preserved within the Waquoit sediments compared with other regional locations such as Salt Pond in Falmouth, MA (i.e. Donnelly et al., 2015) and Succotash in Mattapoisett, MA (i.e. Boldt et al., 2010) could be due to the intensity factor at the time of landfall. Dozens of hurricanes occurred during the historical interval, yet only four were recorded at Succotash, and three in Salt Pond during that time. This indicates that these sites are only sensitive to the most intense hurricanes. If a site is more sensitive to storm events, such as appears to be the case in Waquoit, and records both minor and intense events, it is more difficult to observe significant patterns in representative event beds. The fact that the site is also influenced during both tropical and extratropical storm events further complicates delineating an accurate hurricane chronology and determining storm frequency through time. Sometimes minor and intense events can be distinguished within a particular site (i.e. Lane et al., 2011), based on site specific mechanisms of transport, however this does not appear to be the case in Waquoit.

Additionally, the sensitivity to storm energy within the north basin has likely fluctuated through time, making it difficult to interpret the magnitude and frequency of individual events occurring during the prehistoric period. Within Waquoit Bay, both natural and anthropogenic modifications to tidal inlets have rapidly altered the character of sedimentation within the bay (Aubrey et al., 1993; Maio et al., 2015). The opening and closing of tidal inlets has the potential to rapidly change

the sites sensitivity to increased storm energy (Valiela et al., 1998; Maio et al., 2015). An increased number of active inlets leave back-barrier environments more sensitive to surging storm waters while a more closed system leaves them more protected (Warren and Niering, 1993). For example, the dredging and fortification of the main inlet during the 1930s coupled with the opening of the Eel Pond inlet during the 1938 hurricane had system wide impacts within the estuary, thus altering saltmarsh plant communities (i.e. Orson and Howes, 1992; Aubrey et al., 1993). After this point in time, the system experienced increased sensitivity to storm events which may explain increased residual grain size anomalies in the upper core.

Over longer time-scales, the variability in the position of the barrier beach in relation to the coring location can also affect the sensitivity of back-barrier lagoons, further complicating the sedimentary record of past storm events (Donnelly et al., 2004; Scileppi and Donnelly, 2007). Orson and Howes (1992) proposed that the formation of the Waquoit barrier at its present position did not occur until 1200 ybp. Maio et al. (2014) however, presented evidence that subfossil stumps associated with a back-barrier paleoforest site along the current shoreface of South Cape Beach was in existence prior to 1190 ± 43 cal BP, indicating that the barrier must have been further seaward than today (Maio et al., 2014), thus contradicting previous assertions. This would likely have reduced storm energy reaching the north basin.

5. Conclusions

The brevity of the instrumental record and lack of detailed historical accounts are limiting factors in our understanding of the impact of passing storms on shallow lagoon sediment dynamics. In this study we sought to address this gap in knowledge by deciphering how storm events impact sediment dynamics and hydrographic conditions within Waquoit Bay and generally address the feasibility of developing a hurricane chronology within a shallow groundwater fed coastal lagoon. Challenges in generating a continuous storm chronology exist because of the sites oversensitivity to storm events and the multiple sediment sources and transport pathways.

Sedimentary and radiocarbon evidence presented in this study shows that estuarine conditions have persisted for at least the past 3500 years, with down core fluctuations in grain size distribution indicating both active and quiescent periods within the estuarine facies. The sediment sources and transport mechanisms leading to the coarse grain horizons identified are different than previous paleotempestological studies where sediment transport was mainly seaward to landward as overwash (Liu and Fearn, 2000; Donnelly et al., 2001; Donnelly, 2005; Scileppi and Donnelly, 2007). Rather, this study presents evidence that a strong seaward moving bottom current exists within the north basin thus capable of transporting suspended shoreface sands into the coring site.

Although the stratigraphy of the WAQ cores appear to preserve an archive of past storm events several factors prevent the calculation of hurricane frequencies. These factors include 1) natural and anthropogenic disturbances in the upper meter of sediments, 2) age control (associated with CFAMS method and absence of radioisotope chronomarkers), 3) variable sediment sources and transport mechanisms, 4) sensitivity of site to both tropical and extratropical storms, and 5) changing basin morphology. Despite the limitations in using shallow ground-water fed estuaries for hurricane reconstructions, the results presented here contribute towards the understanding of how these systems respond to storm passage. These results indicate that during storm passage there is significant changes to hydrographic conditions and sediment transport and deposition pathways. With additional age control including more attempts at using radioisotopes and the application of traditional ^{14}C AMS dating, age control could potentially be more tightly constrained and the combined frequencies of extratropical and tropical storm frequencies calculated.

Acknowledgements

We would like to thank Dr. Jon Woodruff from the University of Massachusetts Amherst for his assistance developing the age model, the University of Massachusetts Boston's School for the Environment Graduate Fellowship Program, the Woods Hole Oceanographic Institution Coastal Systems Group Guest Student Program, and the Waquoit Bay National Estuarine Research Reserve for financial and in-kind support. The National Ocean Sciences Accelerator Mass Spectrometry Facility (NOSAMS) at Woods Hole also provided in-kind support. Thanks to P.G. Rosen for her 2003 Master's Thesis which laid the groundwork for this study and the countless others who've supported this project. Vincent Cyrus, Ezrah Pearson, Louis Dogey, Thomas H. Johnson, Vincent, Jane, and Sarah Maio all provided editorial feedback.

References

Aretxabaleta, A.L., Butman, B., Signell, R.P., Dalyander, P.S., Sherwood, C.R., Sheremet, V.A., McGillicuddy Jr., D.J., 2013. Near-bottom circulation and dispersion of sediment containing *Alexandrium fundyense* cysts in the gulf of Maine during 2010–2011. Deep-Sea Res. II Top. Stud. Oceanogr.

Aubrey, D.G., McSherry, T.R., Eliet, P.P., 1993. Effects of multiple inlet morphology on tidal exchange: Waquoit Bay, Massachusetts. Coast. Estuar. Stud. 44, 213–235.

Avila, L.A., Cangialosia, J., 2011. Tropical cyclone report: hurricane Irene: August 21–28, 2011. National Hurricane Center Report AL0920011. U.S. National Oceaninc and Atmospheric Administration's National Weather Service.

Balco, G., Schaefer, J.M., 2006. Cosmogenic-nuclide and varve chronologies for the deglaciation of southern New England. Quat. Geochronol. 1 (1), 15–28.

Bell, E.L., 2009. Cultural resources on the New England coast and continental shelf: research, regulatory, and ethical considerations from a Massachusetts perspective. Coast. Manag. 37 (1), 36.

Blaauw, M., Christen, J.A., 2011. Flexible paleoclimate age-depth models using an autoregressive gamma process. Bayesian Anal. 63 (3), 457–474.

Boldt, K.V., Lane, P., Woodruff, J.D., Donnelly, J.P., 2010. Calibrating a sedimentary record of overwash from southeastern New England using modeled historic hurricane surges. Mar. Geol. 275 (1–4), 127–139.

Boose, E.R., Chamberlin, K.E., Foster, D.R., 2001. Landscape and regional impacts of hurricanes in New England. Ecol. Monogr. 71 (1), 27–48.

Bowen, J.L., Valiela, I., 2001. The ecological effects of urbanization of coastal watersheds: historical increases in nitrogen loads and eutrophication of Waquoit Bay estuaries. Can. J. Fish. Aquat. Sci. 58, 1489–1500.

Brandon, C.M., Woodruff, J.D., Donnelly, J.P., Sullivan, R.M., 2014. How unique was hurricane Sandy? Sedimentary reconstructions of extreme flooding from New York Harbor. Sci. Rep. 4.

Buynevich, I.V., Donnelly, J.P., 2006. Geological signatures of barrier breaching and overwash, southern Massachusetts, USA. J. Coast. Res. Spec. Issue 39, 112–116.

Buynevich, I.V., FitzGerald, D.M., van Heteren, S., 2004. Sedimentary records of intense storms in Holocene barrier sequences, Maine, USA. Mar. Geol. 210 (1), 135–148.

Cronon, W., 2011. Changes in the Land: Indians, Colonists, and the Ecology of New England. Hill and Wang, p. 281.

Dickson, R.R., 1978. Weather and circulation of February 1978; record or near-record cold east of the continental divide with a major blizzard in the northeast. Mon. Weather Rev. 106, 746–751.

Donnelly, J.P., 2005. Evidence of past intense tropical cyclones from backbarrier salt pond sediments: a case study from Isla de Culebrita, Puerto Rico, USA. J. Coast. Res. Spec. Issue 42, 201–210.

Donnelly, J.P., Woodruff, J.D., 2007. Intense hurricane activity over the past 5,000 years controlled by El Nino and the west African monsoon. Nature 447 (7143), 465–468.

Donnelly, J.P., Bryant, S.S., Butler, J., Dowling, J., Fan, L., Hausmann, N., Westover, K., 2001. 700 yr sedimentary record of intense hurricane landfalls in southern New England. Geol. Soc. Am. Bull. 113 (6), 714–727.

Donnelly, J.P., Butler, J., Roll, S., Wengren, M., Webb III, T., 2004. A backbarrier overwash record of intense storms from Brigantine, New Jersey. Mar. Geol. 210 (1), 107–121.

Donnelly, J.P., Hawkes, A.D., Lane, P., MacDonald, D., Shuman, B.N., Toomey, M.R., Woodruff, J.D., 2015. Climate forcing of unprecedented intense-hurricane activity in the last 2000 years. Earth's Future 3 (2), 49–65.

Emanuel, K.A., 1988. The maximum intensity of hurricanes. J. Atmos. Sci. 45 (7), 1143–1155.

Emanuel, K., 2005. Increasing destructiveness of tropical cyclones over the past 30 years. Nature 436 (7051), 686–688.

Emery, K.O., 1969. A Coastal Pond; Studied by Oceanographic Methods. American Elsevier, New York (80 pp.).

Fairbanks, R.G., 1989. A 17, 000-year glacio-eustatic sea level record: influence of glacial melting rates on the Younger Dryas event and deep-ocean circulation. Nature 342 (6250), 637–642.

FitzGerald, D.M., Fenster, M.S., Argow, B.A., Buynevich, I.V., 2008. Coastal impacts due to sea-level rise. Annu. Rev. Earth Planet. Sci. 36, 601–647.

French, K., 2007. A history of trace metal input in an estuary influenced by submarine groundwater discharge: Waquoit Bay National Estuarine Research Reserve - USGS.

Fox, S.E., Teichberg, M., Valiela, I., Heffner, L., 2012. The relative role of niturients, grazing, and predation as controls on macroalgal growth in the Waquoit Bay esturine system. Estuar. Coasts 35, 1193–1204.
Geyer, W., 1997. Influence of wind on dynamics and flushing of shallow estuaries. Estuar. Coast. Shelf Sci. 44 (6), 713–722.
Gontz, A.M., Maio, C.V., Rueda, L., 2013. The Duxbury sunken forest — constraints for local, late Holocene environmental changes resulting from marine transgression, Duxbury Bay, eastern Massachusetts, USA. J. Coast. Res. 29 (6A), 168–176.
Gutierrez, B., Uchupi, E., Driscoll, N., Aubrey, D., 2003. Relative sea-level rise and the development of valley-fill and shallow-water sequences in Nantucket Sound, Massachusetts. Mar. Geol. 193 (3), 295–314.
Hjulstrom, F., 1939. Transportation of detritus by moving water: part 1. Transportation 5-31.
Jelesnianski, C.P., Chen, J., Shaffer, W.A., 1992. SLOSH: Sea, Lake, and Overland Surges from Hurricanes. US Department of Commerce, National Oceanic and Atmospheric Administration, National Weather Service.
Keay, D.L., 2001. A history of Washburn Island. Bridgewater Rev. 20 (2), 22–25.
Kelley, J., Kelley, A., Pilkey Sr., O., 1989. Living With the Maine Coast. Duke University Press, Durham, NC.
Kemp, A.C., Horton, B.P., Culver, S.J., Corbett, D.R., van de Plassche, O., Gehrels, W.R., Parnell, A.C., 2009. Timing and magnitude of recent accelerated sea-level rise (North Carolina, United States). Geology 37 (11), 1035–1038.
Kemp, A.C., Sommerfield, C.K., Vane, C.H., Horton, B.P., Chenery, S., Anisfeld, S., Nikitina, D., 2012. Use of lead isotopes for developing chronologies in recent salt-marsh sediments. Quat. Geochronol. 12, 40–49.
Kirshen, P., Watson, C., Douglas, E., Gontz, A., Lee, J., Tian, Y., 2007. Coastal Flooding in the Northeastern United States Due to Climate Change. 13(2008). Springer, pp. 437–451.
Lane, P., Donnelly, J.P., Woodruff, J.D., Hawkes, A.D., 2011. A decadally-resolved paleohurricane record archived in the late Holocene sediments of a Florida sinkhole. Mar. Geol. 287 (1), 14–30.
Lanesky, D.E., Logan, B.W., Brown, R.G., Hine, A.C., 1979. A new approach to portable vibracoring underwater and on land. J. Sediment. Petrol. 49, 654–657.
Legra, J.C., Safran, R.E., Valiela, I., 1998. Lead concentration as an indicator of contamination history in estuarine sediments. Biol. Bull. 195 (2), 243.
Lima, A.L., Bergquist, B.A., Boyle, E.A., Reuer, M.K., Dudas, F.O., Reddy, C.M., Eglinton, T.I., 2005. High-resolution historical records from Pettaquamscutt River basin sediments: 2. Pb isotopes reveal a potential new stratigraphic marker. Geochim. Cosmochim. Acta 69 (7), 1813–1824.
Little, E.A., 1993. Radiocarbon age calibration at archaeological sites of coastal Massachusetts and vicinity. J. Archaeol. Sci. 20 (4), 457–471.
Little, E.A., 1999. Radiocarbon dating of shell on the southern coast of New England. The Archaeological Northeast. Greenwood Publishing Group, Westport Connecticut, p. 201.
Liu, K.B., Fearn, M.L., 1993. Lake-sediment record of late Holocene hurricane activities from coastal Alabama. Geology 21 (9), 793–796.
Liu, K.B., Fearn, M.L., 2000. Reconstruction of prehistoric landfall frequencies of catastrophic hurricanes in northwestern Florida from lake sediment records. Quat. Res. 54 (2), 238–245.
Ludlum, D.M., 1963. Early American Hurricanes, 1492–1870. Vol. 1. American Meteorological Society, Boston.
Madsen, A.T., Duller, G.A., Donnelly, J., Roberts, H.M., Wintle, A.G., 2009. A chronology of hurricane landfalls at Little Sippewissett Marsh, Massachusetts, USA, using optical dating. Geomorphology 109 (1), 36–45.
Maio, C.V., Gontz, A.M., Tenenbaum, D., 2012. Coastal hazard vulnerability assessment of sensitive historical sites on Rainsford Island, Boston Harbor, Massachusetts. J. Coast. Res. 28 (1), 20–33.
Maio, C.V., Tenenbaum, D.E., Brown, C.J., Mastone, V.T., Gontz, A.M., 2013. Application of geographic information technologies to historical landscape reconstruction and military terrain analysis of an American Revolution Battlefield: Preservation potential of historic lands in urbanized settings, Boston, Massachusetts, USA. J. Cult. Herit. 14 (4), 317–331.
Maio, C.V., Gontz, A.M., Weidman, C.R., Donnelly, J.P., 2014. Late Holocene marine transgression and the drowning of a coastal forest: lessons from the past, Cape Cod, Massachusetts, USA. Palaeogeogr. Palaeoclimatol. Palaeoecol. 393, 146–158.
Maio, C.V., Gontz, A.M., Sullivan, R., Madsen, S., Weidman, C., Donnelly, J.P., 2015. Geologic signatures of storm-driven breaching along a transgressing barrier system, Cape Cod, USA. J. Coast. Res. 32 (2), 264–279.
National Hurricane Center (NHC), 2013. NHC Data Archive Retrieved 12/12/2013, 2013. (from) http://www.nhc.noaa.gov/data/.
National Oceanic and Atmospheric Administration, 2016. Tides and Currents URL: http://tidesandcurrents.noaa.gov/waterlevels.html?id=8447930 (Accessed August 2016).
Nixon, S.W., 1995. Metals Inputs to Narragansett Bay: A History and Assessment of Recent Conditions. Rhode Island Sea Grant, Narragansett, Rhode Island (162 pp.).
Nott, J., 2004. Palaeotempestology: the study of prehistoric tropical cyclones—a review and implications for hazard assessment. Environ. Int. 30 (3), 433–447.
Nott, J., Haig, J., Neil, H., Gillieson, D., 2007. Greater frequency variability of landfalling tropical cyclones at centennial compared to seasonal and decadal scales. Earth Planet. Sci. Lett. 255 (3), 367–372.
Nriagu, J.O., 1998. Tales told in lead. Science 281 (5383), 1622–1623.
Oldale, R.N., 1992. Cape Cod and the Islands: The Geologic Story. Parnassus Imprints East Orleans, Massachusetts.
Oldale, R., O'Hara, C., 1984. Glaciotectonic origin of the Massachusetts coastal end moraines and a fluctuating late Wisconsinan ice margin. Geol. Soc. Am. Bull. 95 (1), 61–74.
Orson, R.A., Howes, B.L., 1992. Salt marsh development studies at Waquoit Bay, Massachusetts: influence of geomorphology on long-term plant community structure. Estuar. Coast. Shelf Sci. 35 (5), 453–471.
Pachauri, R.K., Allen, M.R., Barros, V.R., Broome, J., Cramer, W., Christ, R., Church, J.A., Clarke, L., Dahe, Q., Dasgupta, P., Dubash, N.K., 2014. Climate change 2014: synthesis report. Contribution of working groups I, II and III to the fifth assessment report of the intergovernmental panel on climate change. IPCC, p. 151.
Reimer, P.J., Baillie, M.G., Bard, E., Bayliss, A., Beck, J.W., Blackwell, P.G., Edwards, R.L., 2013. IntCal13 and Marine13 radiocarbon age calibration curves, 0–50,000 years cal BP. Radiocarbon 55 (4), 1869–1887.
Roberts, M.L., von Reden, K.F., Burton, J.R., McIntyre, C.P., Beaupre, S.R., 2011. A gas-accepting ion source for accelerator mass spectrometry: progress and applications. Nucl. Instrum. Methods Phys. Res., Sect. B.
Roberts, M.L., von Reden, K.F., Burton, J.R., McIntyre, C.P., Beaupre, S.R., 2013. A gas-accepting ion source for Accelerator Mass Spectrometry: Progress and applications. Nucl. Instrum. Methods Phys. Res., Sect. B. 294, 296–299.
Rosen, P.G., 2003. The Holocene Evolution of a Shallow Cape Cod Estuary as Preserved in the Sedimentary Record, Waquoit Bay, Massachusetts (Masterrs Masters, State University of New York College at Oneonta, State University of New York College at Oneonta).
Scileppi, E., Donnelly, J.P., 2007. Sedimentary evidence of hurricane strikes in western Long Island, New York. Geochem. Geophys. Geosyst. 8 (6), 1–25.
Snow, E.R., 1943. Great Storms and Famous Shipwrecks of the New England Coast. The Yankee Publishing Company.
Stuiver, M., Braziunas, T.F., 1993. Modeling atmospheric 14C influences and 14C ages of marine samples to 10 000 BC. Radiocarbon 35 (1), 137–189.
Tides and Currents, 2014. Woods Hole, Massachusetts, Station ID: 8447930. (URL:) http://tidesandcurrents.noaa.gov/noaatidepredictions/NOAATidesFacade.jsp?Stationid=8447930.
Uchupi, E., Mulligan, A.E., 2006. Late Pleistocene stratigraphy of upper Cape Cod and Nantucket Sound, Massachusetts. Mar. Geol. 227 (1), 93–118.
USEPA, 2000. National Air Pollutant Emission Trends, 1900–1998. Vol. EPA/454/R-00/002. USEPA, Washington, DC.
Valiela, I., Peckol, P., D'Avanzo, C., Kremer, J., Hersh, D., Foreman, K., Lajtha, K., Seely, B., Geyer, W.R., Isaji, T., Crawford, R., 1998. Ecological effects of major storms on coastal watersheds and coastal waters: hurricane Bob on Cape Cod. J. Coast. Res. 14 (1), 218–238.
Wallace, D.J., Woodruff, J.D., Anderson, J.B., Donnelly, J.P., 2014. Palaeohurricane reconstructions from sedimentary archives along the Gulf of Mexico, Caribbean Sea and western north Atlantic Ocean margins. Geol. Soc. Lond., Spec. Publ. 388 (1), 481–501.
Waquoit Bay National Estuarine Research Reserve (WBNERR), 2016. Accessed June 1, 2016. URL: http://www.waquoitbayreserve.org.
Warren, R.S., Niering, W.A., 1993. Vegetation change on a northeast tidal marsh: Interaction of sea-level rise and marsh accretion. Ecology 74 (1), 96–103.
Woodruff, J.D., Donnelly, J.P., Mohrig, D., Geyer, W.R., 2008. Reconstructing relative flooding intensities responsible for hurricane-induced deposits from Laguna Playa Grande, Vieques, Puerto Rico. Geology 36 (5), 391–394.
Woodruff, J.D., Irish, J.L., Camargo, S.J., 2013. Coastal flooding by tropical cyclones and sea-level rise. Nature 504 (7478), 44–52.